Intracellular calcium strongly potentiates agonist-activated TRPC5 channels

Nathaniel T. Blair, J. Stefan Kaczmarek, and David E. Clapham

Howard Hughes Medical Institute, Department of Cardiology and Manton Center for Orphan Disease, Children's Hospital Boston, and Department of Neurobiology, Harvard Medical School, Boston, MA 02115

TRPC5 is a calcium (Ca^{2+})-permeable nonselective cation channel expressed in several brain regions, including the hippocampus, cerebellum, and amygdala. Although TRPC5 is activated by receptors coupled to phospholipase C, the precise signaling pathway and modulatory signals remain poorly defined. We find that during continuous agonist activation, heterologously expressed TRPC5 currents are potentiated in a voltage-dependent manner (~5-fold at positive potentials and ~25-fold at negative potentials). The reversal potential, doubly rectifying current–voltage relation, and permeability to large cations such as *N*-methyl-D-glucamine remain unchanged during this potentiation. The TRPC5 current potentiation depends on extracellular Ca^{2+}: replacement by Ba^{2+} or Mg^{2+} abolishes it, whereas the addition of 10 mM Ca^{2+} accelerates it. The site of action for Ca^{2+} is intracellular, as simultaneous fura-2 imaging and patch clamp recordings indicate that potentiation is triggered at ~1 µM [Ca^{2+}]. This potentiation is prevented when intracellular Ca^{2+} is tightly buffered, but it is promoted when recording with internal solutions containing elevated [Ca^{2+}]. In cell-attached and excised inside-out single-channel recordings, increases in internal [Ca^{2+}] led to an ~10–20-fold increase in channel open probability, whereas single-channel conductance was unchanged. Ca^{2+}-dependent potentiation should result in TRPC5 channel activation preferentially during periods of repetitive firing or coincident neurotransmitter receptor activation.

INTRODUCTION

Transient receptor potential (TRP) channels are a superfamily of ~28 different proteins present in mammals (Ramsey et al., 2006; Venkatachalam and Montell, 2007). TRP channels have varied expression patterns and biophysical properties, and they have been implicated in a wide range of physiological responses, including sensory transduction pathways involved in temperature, pressure, light, taste, and painful chemical stimuli.

The seven members of the canonical subfamily of TRP channels (TRPC) are most similar to the *Drosophila* TRP channel required in fly vision. All of the TRPC subfamily members are nonselective cation channels with modest Ca^{2+} permeability that, at present, appear to be activated by both G protein–coupled receptors (GPCRs) and growth factor receptors coupled to PLC. The TRPC subfamily can be further divided into TRPC1/C4/C5 and TRPC3/C6/C7. These can form homotetramers, or in some cases heterotetramers, between subfamily members (Strubing et al., 2001, 2003; Hofmann et al., 2002). For the TRPC3/C6/C7 subfamily, activation may be mediated, at least in part, by diacylglycerol released by PLC hydrolysis of phosphatidylinositol 4,5-bisphosphate (PIP_2) into diacylglycerol and inositol tris (1,4,5) phosphate (IP_3). For the TRPC1/C4/C5 subfamily of channels, the intermediates between receptor, PLC activation, and channel activation are not fully understood.

Early work established that in hippocampal neurons, TRPC1/5 heteromers and TRPC5 homomers were expressed in neuronal cell bodies, whereas only TRPC5 homomers were trafficked to neuronal processes (Greka et al., 2003; Bezzerides et al., 2004). We have found no evidence for functional TRPC1 homomeric channels in heterologous expression systems (Strubing et al., 2001, 2003), and the evidence that they exist in native cells is conflicting (Kim et al., 2003; Hartmann et al., 2008). In contrast, TRPC1/4, TRPC1/5, and TRPC4 and TRPC5 homomeric channels clearly exist in both heterologous expression and native tissues.

Modulatory influences on the activity of the TRPC1/C4/C5 subfamily channels have been described, typically for TRPC4 or TRPC5 homomeric channels. These include inhibition of TRPC4 (α isoform) channels by PIP_2 (Otsuguro et al., 2008), inhibition of TRPC5 channels by nucleotides (Dattilo et al., 2008), desensitization of TRPC5 channels by PKC phosphorylation (Zhu et al., 2005), and interaction of both TRPC4 and TRPC5 channels with Ca^{2+} binding proteins. For example,

Correspondence to David E. Clapham:
dclapham@enders.tch.harvard.edu

Abbreviations used in this paper: CCh, carbachol; GPCR, G protein–coupled receptor; HEK, human embryonic kidney; IP_3, inositol tris (1,4,5) phosphate; M1R, muscarinic type 1 receptor; NCS-1, neuronal Ca^{2+} sensor 1; PIP_2, phosphatidylinositol 4,5-bisphosphate; TRP, transient receptor potential.

The Rockefeller University Press $30.00
J. Gen. Physiol. Vol. 133 No. 5 525–546
www.jgp.org/cgi/doi/10.1085/jgp.200810153

calmodulin has been reported to accelerate TRPC5 agonist-activated current (Ordaz et al., 2005), presumably via a direct interaction with the channel; upstream effects via myosin light chain kinase activation have also been reported (Kim et al., 2006; Shimizu et al., 2006). Furthermore, Ca^{2+} binding protein 1 has been reported to inhibit intracellular Ca^{2+} activation of TRPC5 current (Kinoshita-Kawada et al., 2005), whereas neuronal Ca^{2+} sensor 1 (NCS-1) appears to have permissive or stimulatory actions (Hui et al., 2006).

The multitude of Ca^{2+}-dependent effects, causing both stimulation and inhibition, is likely crucial for control of TRPC4 and TRPC5 activity. Thus, a detailed knowledge of the effects of Ca^{2+} on the activity of these channels is important in understanding their potential physiological roles where they are expressed. This includes smooth muscle cells, neuroendocrine cells, and numerous neuronal cell types (Plant and Schaefer, 2005). Here, we focus on TRPC5 homomeric channel currents. We examined the regulation of heterologously expressed TRPC5 activity by intracellular Ca^{2+} using both whole cell and single-channel patch clamp recordings. We find that ~1 μM intracellular [Ca^{2+}] can lead to a 25-fold increase in agonist-activated TRPC5 current at physiological voltages, likely resulting from an increase in channel open probability.

MATERIALS AND METHODS

Cell culture and transfection

Human embryonic kidney (HEK) cells were cultured in a 1:1 mixture of DMEM/F-12 medium supplemented with 10% fetal bovine serum at 37°C with 5% CO_2 (Invitrogen). Cells were passaged 6–24 h before transfection and transfected in 35-mm dishes using 5 μl Lipofectamine 2000 (Invitrogen) with 1–1.5 μg of mouse TRPC5 (in pCI-neo) or mouse TRPC5-GFP (in pIRES, after excision of internal ribosomal entry site to generate a C-terminal fusion of TRPC5 and GFP [Bezzerides et al., 2004]) and 0.8 μg of human muscarinic type 1 receptor (M1R; in pcDNA3). 0.05–0.1 μg eGFP-C1 or 0.25 μg DsRed-N1 (for fura-2 imaging experiments) was used as a transfection marker (Clontech Laboratories, Inc.). In experiments where mutant calmodulin with all four E-F hands disrupted (CaM1234) was used (Fig. 14), 1.64 μg CaM1234/pcDNA3zeo was included with the above plasmids. After 2–4 h of transfection, fresh media was added. 12–24 h later, the cells were plated onto glass coverslips. Recordings were made up to 8 h after plating. For inside-out single-channel recordings, coverslips were coated with 0.1 mg/ml poly-L-lysine to improve cell adhesion and subsequent patch excision.

Electrophysiology

Whole cell and single-channel currents were recorded using Axopatch 200A and 200B amplifiers, acquired and controlled using a Digidata 1320A and pClamp 9 (MDS Analytical Technologies). Analysis was typically performed in IGOR Pro 5 (Wavemetrics) and Prism 4 (Graphpad). Single-channel analysis was performed in pClamp 9. Pipettes were pulled from borosilicate glass capillaries (WPI or A-M Systems), had resistances of 2–4 MΩ for whole cell recordings and 4–7 MΩ for single-channel recordings, and were wrapped with parafilm near their tips to reduce capacitance. Whole cell currents were filtered at 5 kHz (4-pole low-pass Bessel) and sampled at 20 kHz. During whole cell recordings the capacity current was minimized by amplifier circuitry, and the series resistance was compensated by 85%. We found that the strongly outwardly rectifying TRPC5 current was sensitive to the series resistance remaining after compensation. Thus, outward currents were analyzed only in cells where the initial uncompensated series resistance was <10 MΩ. To calculate the current density, cell capacitance was either measured from the uncompensated response to −10-mV pulses (average of 8–14 sweeps acquired at 50 at 10 kHz bandwidth) or from the capacitance value on the amplifier after compensation. All voltages were corrected for the −11- or −13-mV measured junction potentials present between the internal solutions and the 2 Ca external solution present before seal formation. Experiments were performed at room temperature (21–24°C).

TRPC5 currents were elicited by voltage ramps consisting of a 40-ms step to −100 mV, followed by a 200-ms ramp to +100 mV, 40 ms at +100 mV, and finally a 20–40-ms step to −60 mV. Voltage ramps were applied at 0.5 Hz from a holding potential of −40 mV. Inward currents were the average of 25 ms during the holding potential preceding each ramp; we chose this potential to minimize the contribution of a contaminating Cl^- current (reversal potential ~−53 mV), which was occasionally recorded in cells using high internal [Ca^{2+}]. Due to constitutive TRPC5 activity, currents were not typically leak subtracted; however, constitutive current was absent in recordings made using internal solutions with free <350 nM [Ca^{2+}] in nominally Ca-free external solutions without agonist. In these cases (i.e., Figs. 6, 12, and 13), the inward current was leak subtracted with the average of four to eight sweeps, recorded in nominally Ca^{2+}-free external solution before carbachol (CCh) addition.

To examine possible changes in instantaneous I-V relation for TRPC5 channels during potentiation by Ca^{2+} (Fig. 9), we used two protocols that gave similar results. In both, voltage steps to a conditioning potential of either +90 (for 50 ms) or +100 mV (for 15 ms) activated TRPC5 channels, and then tail currents were measured from 0.7 to 0.85 ms after repolarization to potentials ranging from −120 through +100 mV. In one set of experiments, repolarization was to −120, −90, −60, −30, and +60 mV for 40 ms. These were applied in a single sweep immediately after one another; sweep to sweep onset was 1 Hz. In another set of experiments, repolarization was to −100 to +100 mV (in 5-mV increments) for 50 ms; sweep to sweep onset was 2 Hz.

Solutions

The standard Cs-Asp internal solution contained (in mM): 150 Cs-aspartate, 2 $MgCl_2$, 0.36 $CaCl_2$, 1 EGTA, 4 MgATP, 0.3 NaGTP, and 10 HEPES, pH 7.20 with CsOH (calculated free [Ca^{2+}] = 100 nM). In several experiments, we varied the amount of $CaCl_2$ and buffer added to internal solutions to set free [Ca^{2+}] to different values; the precise components of each internal solution are noted in the figure legends. The free [Ca^{2+}] for all internals was calculated using WebMaxChelator (http://www.stanford.edu/~cpatton/maxc.html), assuming an ionic strength of 0.16. The standard external solution ("2 Ca external") contained (in mM): 150 NaCl, 4 KCl, 2 $CaCl_2$, 1 $MgCl_2$, 10 HEPES, and 10 D-glucose, pH 7.40, with NaOH. 2 Ba external solution was identical, except 2 mM $BaCl_2$ replaced the $CaCl_2$. "Nominally Ca-free" external solution contained (in mM): 150 NaCl, 4 KCl, 3 $MgCl_2$, 10 HEPES, and 10 D-glucose, pH 7.40, with NaOH. In some experiments (e.g., Fig. 12), the concentrations of divalent cations Ca^{2+} and Mg^{2+} were varied; again, the solution composition is noted in the figure legend.

Single-channel analysis

Single-channel currents were filtered with a 4-pole low-pass Bessel filter at 2 kHz and sampled at 50 kHz. Recordings were converted to idealized traces using pClamp 9 software, including only events

that were >0.5 times the mean amplitude. We assumed a dead time of 0.25 ms. TRPC5 channel openings had single-channel conductances of ~40–50 pS; in some excised patches we observed a smaller amplitude opening of 17.6 ± 1.1 pS (n = 5). We omitted these lower conductance channel-containing patches from analyses.

Calcium imaging

DsRed-positive cells were loaded with 100 µM fura-2 (pentapotassium salt) via the patch pipette. Cells were held at −40 mV, and the typical voltage ramp protocol was applied at 0.2 Hz. Immediately before each voltage ramp, cells were alternatively illuminated with 340 and 380 nm light (Lambda DG-4; Sutter Instrument Co.) for 100–200 ms, and the emission light >510 nm was captured using a CCD camera (Orca-ER; Hamamatsu Photonics) and analyzed with Slidebook (Intelligent Imaging Innovations) or Metamorph (MDS Analytical Technologies). After background subtraction, the ratio of the 340- and 380-nm excited images was calculated and converted to free $[Ca^{2+}]$ using: $[Ca^{2+}] = K^*(R_{max}-R)/(R-R_{min})$, where K^* = 2.7536 µM, R_{max} = 12.4, and R_{min} = 0.3. These values were calculated from average values measured using internal solutions with varying $[Ca^{2+}]$ in untransfected HEK cells as described by Neher (2005).

Chemicals

BAPTA tetracesium salt and fura-2 pentapotassium salt were purchased from Invitrogen. Calmodulin inhibitory peptide and W-7 were from EMD. Stock solutions were prepared in water (calmodulin inhibitory peptide) or DMSO (W-7) and diluted fresh daily into the internal solution at the indicated concentrations. All other reagents were from Sigma-Aldrich.

Data analysis

Averaged results are presented as mean ± SEM. Population means were tested for significance with Student's two-tailed t test, with $P < 0.05$ considered significant.

RESULTS

Agonist stimulation of M1Rs leads to biphasic activation of TRPC5 channels

Fig. 1 shows the typical currents evoked by voltage ramps in a HEK cell transiently transfected with mouse TRPC5 and the human M1R, recorded using internal solutions with modest Ca^{2+} buffering (1 mM EGTA). The initial constitutive currents were quite small, with an average current density at −40 mV of −1.4 ± 0.2 pA/pF (n = 30), but outwardly rectifying currents at +100 mV (20.0 ± 2.6 pA/pF) indicated the presence of TRPC5 channels. Upon the addition of 100 µM CCh to activate M1Rs, a current with the characteristic TRPC5 I-V relationship immediately began to develop; the inward current was roughly constant from −100 to −50 mV and declined as the reversal potential (~−5 mV in our solutions) was approached. At potentials positive to the reversal potential, the current was small and flat until +40 mV, whereupon the current became large and relatively linear (Okada et al., 1998; Schaefer et al., 2000; Strubing et al., 2001).

The TRPC5 current amplitudes steadily increased over ~60 s after CCh application, until the rate of current change dramatically accelerated, reaching a plateau at +100 mV (8.7-fold increase in current). The inward current at −40 mV increased to an even larger degree (17.9-fold), reaching its new peak 10 s later than the +100-mV peak. Despite the large current increase, the reversal potential did not change and the flat portion of the current voltage from 0 to +40 mV remained.

The different kinetics of current increase at +100 and −40 mV are more obvious when the absolute value of the ratio between these currents is calculated (Fig. 1 B). This ratio initially increased sharply soon after CCh addition, as the outward current developed before the inward. After ~30 s it reached a new value where the current at +100 mV was ~16-fold larger than that at −40 mV. However, as the CCh application continued, the rectification ratio steadily increased until a rapid increase led to a peak where the outward current was ~67-fold larger than the inward. This large asymmetry in the inward and outward currents was maintained for only a short time, as over the next 14 s the ratio declined to ~7.3, lower than that achieved before the rapid increase in current level.

This biphasic activation, with a delayed, sudden increase in TRPC5 current, was observed in 18 of 30 cells recorded with an internal solution containing 100 nM of calculated free $[Ca^{2+}]$ and 1 mM EGTA. These cells had peak current densities at −40 mV ranging from −39 to −512 pA/pF (mean −153.0 ± 27.2 pA/pF). The latency from CCh addition to the peak current in these 18 cells varied from 10 to 88 s, with some cells showing a nearly immediate current increase, whereas in others it developed more slowly (average 38.3 ± 5.5 s; Fig. 1 C). The current at +100 mV consistently reached its new peak 2–10 s before the peak current measured at −40 mV. In the remaining 12 cells, the TRPC5 current activated with an approximately single-exponential time course before reaching steady state at −5.1 ± 0.8 pA/pF at −40 mV (−10.6 pA/pF maximum) for the duration of CCh application (typically 60–90 s). A similar delayed increase in TRPC5 currents activated by the histamine type 1 receptor or internal GTP-γ-S has been reported by Obukhov and Nowycky (2004, 2008), suggesting that the response is not unique to the M1R.

Delayed potentiation of agonist-activated TRPC5 channels requires elevation of intracellular $[Ca^{2+}]$

TRPC5 channels are Ca^{2+} permeable, with reported relative permeabilities of Ca^{2+} to Na^+ (P_{Ca}/P_{Na}) ranging from 1 to 14 (Plant and Schaefer, 2005). Thus, the large amplitude currents we recorded suggest that significant Ca^{2+} entry occurred. This Ca^{2+} entry might escape the buffering of the low concentrations of EGTA we used in our internal solution for Fig. 1. Thus, the delayed increase in TRPC5 current could reflect a Ca^{2+} dependence of TRPC5 channels themselves or other components of the agonist activation pathway. If this increase is Ca^{2+} dependent, increasing the buffering capacity of the internal

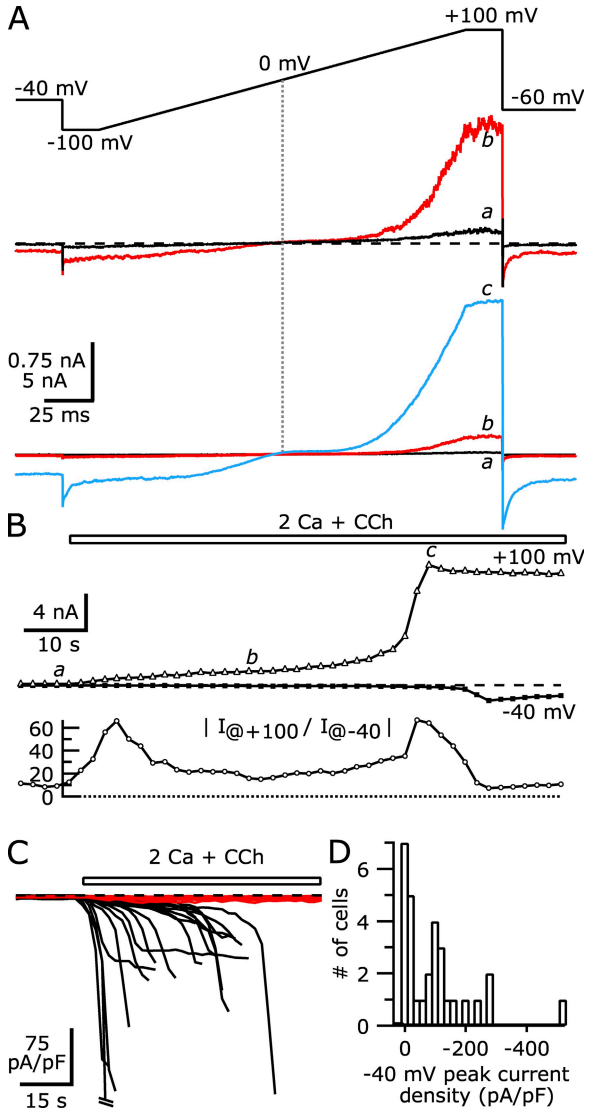

Figure 1. The activation of heterologously expressed TRPC5 channels by M1R stimulation is biphasic. (A) TRPC5 currents evoked by stimulation of M1Rs with 100 μM CCh were elicited by 200-ms voltage ramps from −100 to +100 mV, applied at 0.5 Hz from a holding potential of −40 mV. (Top) Ramp currents recorded before (*a*) and 30 s after CCh addition (*b*) are shown. (Bottom) After 60 s in CCh (*c*), the TRPC5 current suddenly increased ∼8.7-fold at +100 mV compared with *b*. The vertical scale bar corresponds to 0.75 nA in the top currents and 5 nA for the bottom. The dashed line indicates zero current level in this and all other figures. (B; Top) The current at +100 mV (open triangles, 5 ms average at end of ramp) and −40 mV (closed circles, 25 ms averaged immediately before ramp) are plotted. The open bar indicates the timing of the application of 100 μM CCh. (Bottom) The rectification of the TRPC5 current, calculated as the absolute value of the current at +100 mV divided by the current at −40 mV, is plotted (open circles). (C) Average current density at −40 mV evoked by 100 μM CCh is shown for 30 TRPC5/M1R-expressing cells. For clarity, traces are truncated after the peak current density; the peak of one cell is truncated by the vertical scale. Cells that displayed biphasic activation (18 of 30) are shown in black, whereas cells that displayed a single phase of activation (12 of 30) are shown in red. (D) Histogram of peak current density at −40 mV after CCh addition in TRPC5-expressing cells. Internal solution (in mM): 150 Cs-Asp, 2 $MgCl_2$, 0.36 $CaCl_2$, 1 EGTA, 4 MgATP, 0.3 NaGTP, and 10 HEPES, pH 7.20 with CsOH. External solution: 2 Ca external.

solution might slow or prevent the TRPC5 current potentiation. Fig. 2 A shows the current densities of eight cells measured at −40 mV, recorded using Cs-Asp internal solution with calculated free [Ca^{2+}] maintained at 100 nM with 10 mM EGTA. Four of these cells had peak current densities at −40 mV of −14.2 pA/pF or less (−10.9 ± 2.1 pA/pF), similar to cells in Fig. 1 C that did not undergo potentiation. The activation of the current in these four cells followed a similar single-exponential time course. In contrast, the currents at −40 mV from the remaining four cells reached peak densities ranging from −46.8 to −498.6 pA/pF (−244.3 ± 95.1 pA/pF), similar to the cells that underwent potentiation in Fig. 1 C. The latency to peak in these cells was increased with 10 mM EGTA in the internal solution and ranged from 56 to 168 s after CCh application. This increase presumably resulted from the requirement for more Ca^{2+} entry before escape from Ca^{2+} buffer control.

BAPTA and EGTA have similar K_Ds for Ca^{2+} binding, but BAPTA buffers ∼200-fold more rapidly (Naraghi, 1997). Thus, BAPTA can more effectively reduce [Ca^{2+}] at small time and spatial scales near Ca^{2+} entry points (Neher, 1998). When TRPC5/M1R-expressing cells were recorded using a Cs-Asp internal solution (100 nM of calculated free [Ca^{2+}] now buffered with 10 mM BAPTA), we found that the current amplitudes were small and no delayed current potentiation occurred. Fig. 2 B shows the current densities at −40 mV for nine cells recorded with this internal solution: currents activated with a single-exponential time course that reached an average peak amplitude of −6.3 ± 1.4 pA/pF. This result suggests that tight control of [Ca^{2+}] close to Ca^{2+} entry sources by BAPTA can effectively prevent TRPC5 potentiation.

BAPTA itself might limit agonist-dependent signaling by inhibiting PLC (Hardie, 2005). To determine whether the reduction of TRPC5 current by high internal BAPTA results from this inhibition or from its fast Ca^{2+} buffering, we compared the responses in Fig. 2 B to recordings of TRPC5/M1R-expressing cells (1 mM EGTA in the internal solution) when the CCh concentration was reduced to 10 μM (not depicted). Previous work demonstrated that heterologously expressed M1Rs activated with 10 μM CCh should result in ∼40–50% less PIP_2 hydrolysis than with 100 μM CCh (Biddlecome et al., 1996; Willars et al., 1998). Out of 20 cells recorded in this way, 10 displayed biphasic activation with large current amplitudes (average current density at −40 mV = −140.4 ± 28.6 pA/pF), whereas the remaining cells had small current amplitudes (average of −5.7 ± 0.6 pA/pF; n = 10). Thus, despite a lower level of agonist stimulation at M1R receptors, a large fraction of TRPC5/M1R-expressing

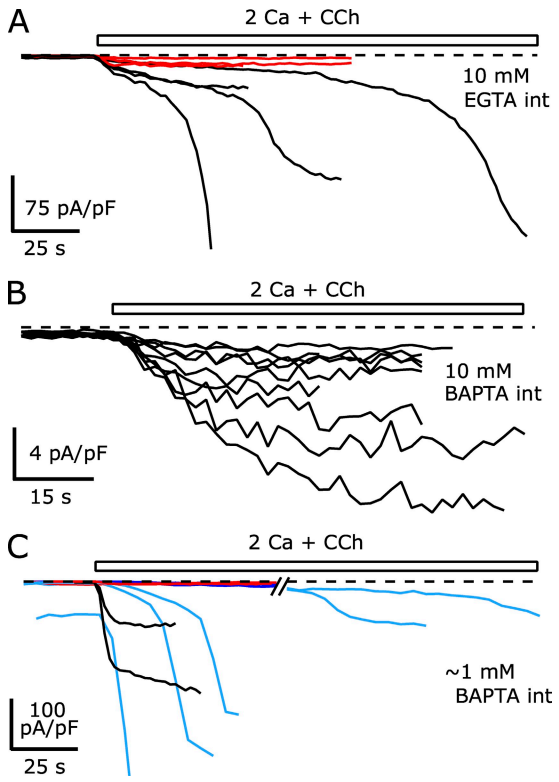

Figure 2. Increased internal Ca^{2+} buffering slows or prevents the delayed increase in CCh-activated TRPC5 current. The calculated free [Ca^{2+}] for all internal solutions was ~100 nM. The TRPC5 I-V curves were not affected by the composition of these internal solutions. (A) The average −40-mV current densities of eight cells recorded using an internal solution containing (in mM): 150 Cs-Asp, 2 $MgCl_2$, 3.62 $CaCl_2$, 10 EGTA, 4 MgATP, 0.3 NaGTP, and 10 HEPES, pH 7.20 with CsOH. The four cells where the peak current density at −40 mV remained less than −15 pA/pF during the CCh application are shown in red. (B) The average −40-mV current densities from nine cells recorded using an internal solution containing (in mM): 110 Cs-Asp, 10 CsCl, 2 $MgCl_2$, 3.10 $CaCl_2$, 10 Cs_4-BAPTA, 4 MgATP, 0.3 NaGTP, and 10 HEPES, pH 7.20 with CsOH. (C) The average −40-mV current densities of nine cells recorded using either an internal solution containing (in mM): 146 Cs-Asp, 2 $MgCl_2$, 0.31 $CaCl_2$, 1 Cs_4-BAPTA, 4 MgATP, 0.3 NaGTP, and 10 HEPES, pH 7.20 with CsOH (shown as black traces), or 145 Cs-Asp, 2 $MgCl_2$, 0.307 $CaCl_2$, 0.99 Cs_4-BAPTA, 0.1 fura-2 (pentapotassium salt), 4 MgATP, 0.3 NaGTP, and 10 HEPES, pH 7.20 with CsOH (shown as blue traces). The two cells where peak current density at −40 mV remained less than −2.3 pA/pF are shown in red (the same fura-2–free internal solution as above). 95 s have been omitted from the trace to show the long latency peaks in two cells. External solution: 2 Ca external solution for each.

cells can still undergo potentiation with low internal Ca^{2+} buffering. This suggests that the suppression of potentiation by 10 mM BAPTA is likely the result of its ability to rapidly buffer Ca^{2+} entering the cell.

When the BAPTA concentration in the internal solution was reduced to ~1 mM and Ca^{2+} was added to give 100 nM of calculated free [Ca^{2+}], the resulting TRPC5 current amplitudes were similar to those recorded with 1 mM EGTA (Fig. 2 C). In nine cells recorded with ~1 mM BAPTA in the internal (three with 1 mM BAPTA and six with 0.99 mM BAPTA + 100 µM fura-2), seven cells had peak current densities at −40 mV from −31.9 to −417 pA/pF (−116 ± 52.3 pA/pF), with latencies from 20 to 270 s. The two other cells had small CCh-elicited currents after reaching steady state (−2.0 and −2.3 pA/pF). The long latencies in two cells (220 and 270 s) possibly resulted from the slower application of ramp voltages used in BAPTA/fura-2 experiments (0.2 Hz vs. the 0.5 Hz used in all other experiments). Ca^{2+} entry might be enhanced during the hyperpolarizing portion of the voltage ramp, and slower application of ramp stimuli likely resulted in a slower intracellular [Ca^{2+}] elevation.

The fact that increasing the Ca^{2+} buffering capacity of the internal solution slows or prevents the sudden potentiation of the TRPC5 current suggests that potentiation requires an increase in intracellular [Ca^{2+}]. In these HEK cells, Ca^{2+} presumably enters through TRPC5 channels, but it might also be released from endoplasmic reticular stores in response to IP_3. To determine if Ca^{2+} entry is required for the potentiation of TRPC5 channels, we tested whether the removal of external Ca^{2+} can prevent or reverse the delayed increase in CCh-activated TRPC5 current (Fig. 3). For these experiments, we used a Cs-Asp internal solution with 100 nM of calculated free [Ca^{2+}] using 1 mM BAPTA. As shown for the cell in Fig. 3 A, voltage ramps applied before the addition of CCh elicited a small constitutive TRPC5 current that was strongly reduced after the external solution was switched to nominally Ca-free external solution with 3 mM $MgCl_2$ (51% reduction in current at +100 mV; 86% reduction in current at −40 mV). This reduction was complete within the 2 s between applied voltage ramps and likely resulted from a decrease in the potentiation of TRPC5 channels due to extracellular Ca^{2+} binding at a site in the presumed S5-pore linker region of the channel (Jung et al., 2003). This site is formed by a series of acidic residues and binds not only Ca^{2+} but also lanthanides (lanthanum and gadolinium) to increase channel open probability in a voltage-dependent manner. Constitutive TRPC5 current in the absence of agonist might result from constitutive activity of the overexpressed M1Rs (e.g., recruitment of PLC by Gβγ despite low Ca^{2+} concentrations [Drin and Scarlata, 2007]) or of PLC itself.

The application of 100 µM CCh in nominally Ca-free external solution to the cell shown in Fig. 3 (A–C) activated TRPC5 current with a single-exponential time course, reaching a steady-state amplitude of 2,100 pA at +100 mV and −22 pA at −40 mV. Over the course of the 60-s CCh application, the TRPC5 current remained constant and never exhibited spontaneous potentiation. When the extracellular solution was switched to 2 Ca external solution (still with 100 µM CCh), both the inward and outward current immediately increased, again,

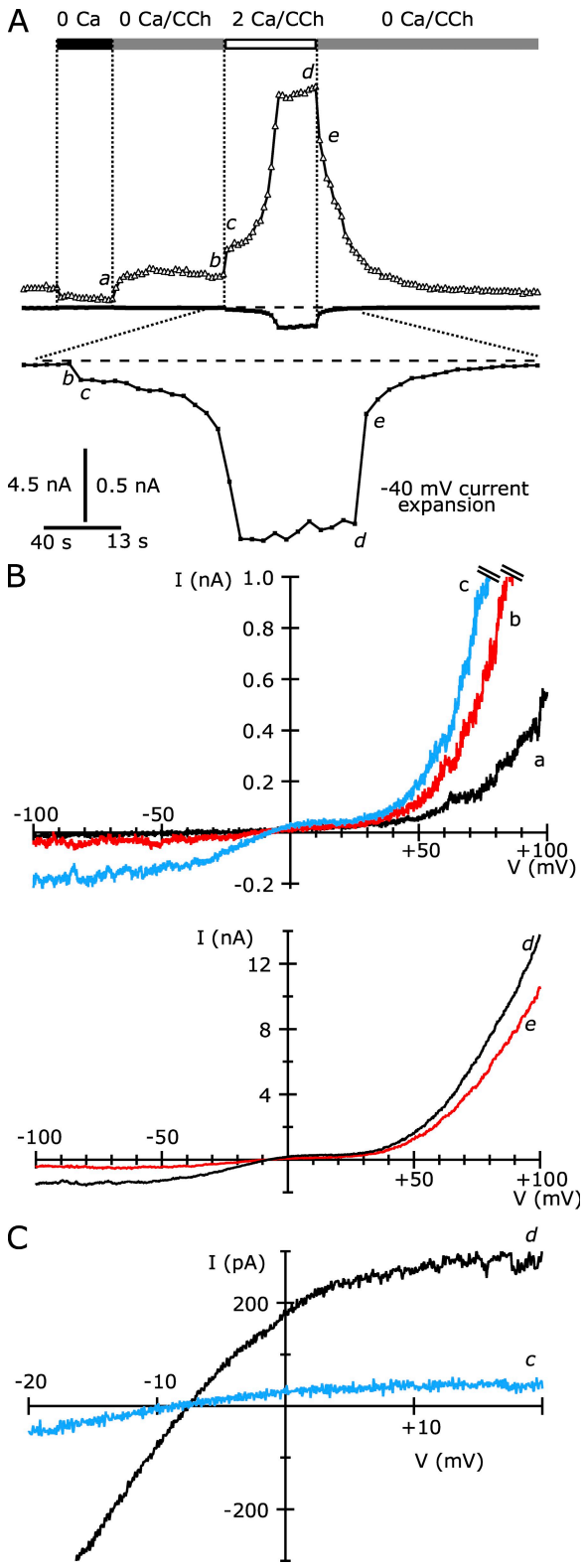

Figure 3. Removal of extracellular Ca^{2+} abolishes large-amplitude CCh-activated currents in TRPC5/M1R-expressing cells. (A; Top) The average currents at +100 mV (triangles) and −40 mV (squares) recorded during the application of ramp voltage stimuli in the presence of the external solutions indicated by the bars. The black bar indicates nominally Ca-free external, the gray bar indicates nominally Ca-free external with 100 μM CCh, and the open bar indicates 2 Ca external solution with 100 μM CCh. (Bottom) The average TRPC5 current at −40 mV on an expanded scale. The lowercase letters indicate the timing of the I-V curves elicited by voltage ramps shown in B. (B) I-V curves for TRPC5 current elicited by voltage ramps before (top) and after (bottom) potentiation. Note that the currents above 1 nA (∼+60 to +100 mV) are not shown (hatched bars; these currents continue upward at the same slope without saturation). (C) I-V curves near the TRPC5 reversal potential are shown immediately after the addition of external Ca^{2+} (*c*) and 48 s after current had reached the potentiated plateau (*d*) on an expanded scale to show reversal potentials. Internal solution (in mM): 150 Cs-Asp, 2 $MgCl_2$, 0.31 $CaCl_2$, 1 Cs_4-BAPTA, 4 MgATP, 0.3 NaGTP, and 10 HEPES, pH 7.20 with CsOH. External solution: 2 Ca and nominally Ca-free external solutions had 1 and 3 mM $MgCl_2$, respectively.

likely due to potentiation at the extracellular Ca^{2+}/lanthanide site (Fig. 3 B). Over the course of the next 28 s, the current further increased, reaching a plateau that was largely maintained while extracellular Ca^{2+} was present. At this point, the peak current at +100 mV was approximately eightfold larger relative to the current recorded immediately after Ca^{2+} readdition; the inward current at −40 mV was ∼18-fold larger. Removal of external Ca^{2+} reversed the current potentiation, with the current immediately falling after Ca^{2+} removal, and continuing to decline over the next ∼90 s. The TRPC5 current finally reached a new steady-state amplitude that was smaller than the initial amplitude of the CCh-activated current in nominally Ca-free external solution. This reduction might result from a desensitization of the overall response, arising either from reductions in the activity of TRPC5 channels themselves or other components of the signaling pathway (e.g., receptors, heterotrimeric G proteins, or PLC). A subsequent readdition of extracellular Ca^{2+} (still with CCh) in this cell generated another similar response, with an immediate increase in TRPC5 current amplitude followed by a delayed peak. Although the peak currents after the first external Ca^{2+} addition were 8–18-fold larger than currents recorded immediately after the return to 2 Ca external solution, they retained the reversal potential and flat portion of the TRPC5 I-V relation from 0 to +40 mV (Fig. 3 C). Also, removal of external Ca^{2+} after CCh activation of TRPC5 did not cause a change in the reversal potential, strongly suggesting that the effects occur by altering the activity of TRPC5 channels and not unrelated conductances.

We quantified the extent of Ca^{2+} potentiation of TRPC5 current as the peak amplitude in 2 Ca external solution relative to the amplitude immediately after Ca^{2+} readdition. From eight TRPC5/M1R-expressing cells recorded in this way (i.e., as in Fig. 3 A), the average potentiation of the current at +100 mV was 4.75 ± 0.62-fold. In contrast, the inward current at −40 mV was potentiated to a much greater extent, with the peak current 24.0 ± 8.5-fold larger. Replacement of external

Ca^{2+} with Ba^{2+} also led to a reversal of TRPC5 current potentiation (e.g., Fig. 9 B), similar to Mg^{2+} replacement. The greater potentiation of inward current relative to outward current resulted in a more linear I-V relation (the flat portion positive to the reversal potential was maintained). A similar finding was recently reported by Obukhov and Nowycky (2008).

Although 18 of 30 TRPC5/M1R-expressing cells recorded in weakly buffered internal Ca^{2+} underwent potentiation, the 12 cells that did not undergo potentiation might have had lower expression levels that resulted in insufficient Ca^{2+} entry. Alternatively, modulatory processes might have prevented the ability of TRPC5 channels in this subset of cells from responding to any increase in intracellular [Ca^{2+}]. To distinguish between these alternatives, we increased the calcium in the external solution to 10 mM for cells that failed to undergo potentiation after initial activation by 100 µM CCh in 2 Ca external solution. As shown in Fig. 4 (A and B), application of 10 Ca external solution rapidly, but not immediately, induced potentiation. The current increased over 8 s to a level approximately sevenfold greater than in 2 Ca external solution, and this level was maintained. Interestingly, returning cells to 2 Ca external did not abolish the potentiation, suggesting that the increased TRPC5 current after potentiation might have been sufficient to maintain high intracellular [Ca^{2+}] and potentiation.

In 13 of 15 TRPC5/M1R-expressing cells treated in this manner, we observed potentiation of the current after extracellular perfusion of 10 Ca external solution and CCh (Fig. 4 C). The average current density at −40 mV in 2 Ca external solution was −7.3 ± 1.2 pA/pF, which increased to a peak of −70.1 ± 10.6 pA/pF (n = 13) after external [Ca^{2+}] was increased to 10 mM. The average potentiation of the current at −40 mV was 14.6 ± 2.7-fold (n = 13; Fig. 4 D). As shown in Fig. 4 C, the latency to peak current after the addition of 10 Ca external solution was bimodal: in 7 of the 13 cells the peak occurred 8.3 ± 1.0 s (n = 7) after 10 mM Ca^{2+} application, whereas in the remaining 6 cells the peak occurred with a significantly longer latency of 44.0 ± 4.7 s. Both values are longer than the solution exchange time and presumably reflect the time course of the intracellular [Ca^{2+}] rise.

We tested whether a different Gαq/11-coupled receptor can lead to potentiation of TRPC5 currents. Coexpression of the mGluR1 receptor with TRPC5 channels and activation by 100 µM (RS)-3,5-dihydroxyphenylglycine alone did not result in potentiation in five tested cells, likely due to the resulting small currents (−1.35 ± 0.28 pA/pF at −40 mV, not depicted). However, subsequent application of 10 Ca external solution potentiated TRPC5 currents in four of the five TRPC5/mGluR1-expressing HEK cells, on average 22.6 ± 4.3-fold (the remaining cell current did not change). The latency to peak was much longer in these cells (101.8 ± 31.7 s; n = 4) than in the M1R-expressing cells after the addition of 10 Ca external. The reasons for such large differences in current activation by the two receptors are unclear, but they might reflect differing expression levels or receptor-dependent modulatory effects. However, Ca^{2+} potentiation can occur in response to the activation of multiple Gαq/11-coupled receptors.

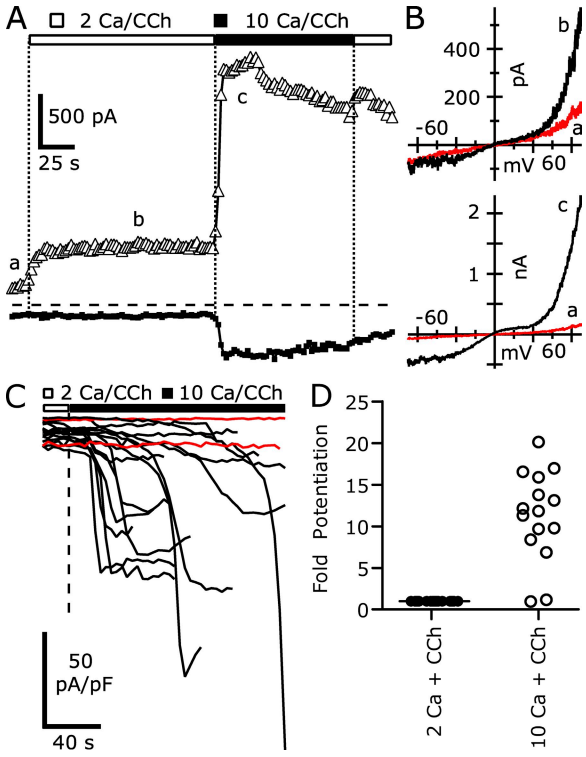

Figure 4. The application of 10 mM of extracellular Ca^{2+} rapidly induces large-amplitude TRPC5 currents in TRPC5 and M1R cotransfected HEK cells. (A) The average TRPC5-mediated currents at +100 mV (triangles) and at −40 mV (squares). Open and black bars indicate the timing of the addition of external solution. (B) I-V curves taken from ramps applied at the times shown by the lowercase letters in A. Currents before (top) and after (bottom) potentiation are shown. (C) The average current densities at −40 mV of 15 cells in response to 10 Ca external; before calcium increase, the bath contained 2 Ca external solution + 100 µM CCh. Cells that were potentiated are shown in black, and unpotentiated cells are shown in red. (D) Potentiation of current at −40 mV in 10 Ca^{2+} external (right) relative to 2 Ca external. Internal solution (in mM): 150 Cs-Asp, 2 $MgCl_2$, 0.36 $CaCl_2$, 1 EGTA, 4 MgATP, 0.3 NaGTP, and 10 HEPES, pH 7.20 with CsOH (100 nM calculated free [Ca^{2+}]). External solution: 2 or 10 Ca external, both with 1 mM $MgCl_2$.

Intracellular [Ca^{2+}] above 1 µM maximally potentiates agonist-activated TRPC5 channels

Our results indicate that a rise in intracellular [Ca^{2+}] is required to potentiate TRPC5 current, but its detailed concentration dependence is unclear. Overexpression of TRPC5 channels might lead to non-physiological [Ca^{2+}] after the activation of M1Rs. To determine the range of

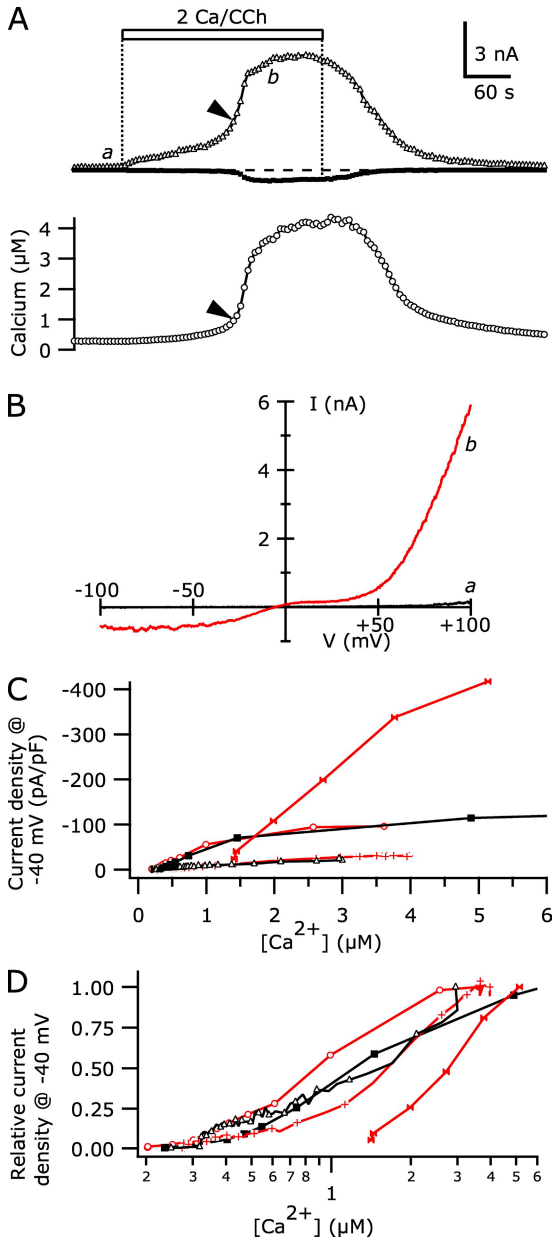

Figure 5. TRPC5 current increases occur with intracellular [Ca^{2+}] at ~1 μM. (A; Top) The average currents at +100 mV (triangles) and −40 mV (squares) recorded during repetitive voltage ramp stimuli applied at 0.2 Hz during the addition of 100 μM CCh in 2 Ca external (open bar). (Bottom) Intracellular [Ca^{2+}] monitored by fura-2 fluorescence recorded in the same cell. The arrowheads indicate the point at which the time derivative of the current at −40 mV reached 50% of its maximum. (B) I-V curves for current before (*a*) and during (*b*) the peak response to CCh application. (C) The current densities at −40 mV from CCh application to the peak value are plotted versus intracellular [Ca^{2+}] for five cells that underwent potentiation. The time between symbols is 4 s for each cell, so that traces with more symbols represent cells with greater latencies to peak (e.g., latency to peak current was 48 s in the cell shown by open circles, whereas it was 216 s in the cell shown by open triangles). The [Ca^{2+}] axis is truncated above 5 μM. The cell in A is shown by plus signs. Alternating cells are shown in red and black for clarity. (D) Current densities at −40 mV from C are normalized to their peak values and plotted against [Ca^{2+}] on a log-scale (symbols correspond to the same cells). For clarity, cells with long peak latencies (shown as open triangles and plus signs) have only every third symbol displayed. Internal solution (in mM): 146 Cs-Asp, 2 $MgCl_2$, 0.31 $CaCl_2$, 0.99 Cs_4-BAPTA, 0.1 fura-2, 4 MgATP, 0.3 NaGTP, and 10 HEPES, pH 7.20 with CsOH.

intracellular [Ca^{2+}] required for TRPC5 potentiation, we recorded TRPC5 currents and monitored intracellular [Ca^{2+}] using 100 μM fura-2 added to the internal solution (~100 nM of calculated free [Ca^{2+}] with 0.99 mM BAPTA). Fig. 5 shows the currents and the calculated [Ca^{2+}] recorded from one such TRPC5/M1R-expressing cell after the application of 100 μM CCh. Both the TRPC5 current at −40 mV and intracellular [Ca^{2+}] initially increased slowly, but after 150 s in CCh the rise in the current and intracellular [Ca^{2+}] accelerated. At the point where the time derivative (dI/dt) of the current at −40 mV reached 50% of its maximum, the calculated free [Ca^{2+}] was 945 nM (in this cell). As the CCh application continued, TRPC5 current and [Ca^{2+}] increased further until both reached a plateau. The fura-2 signal indicated that [Ca^{2+}] was ~4 μM at this point, although with its high affinity (K_D ~250 nM) the fura-2 was very likely saturated, and real intracellular [Ca^{2+}] might have been even higher. It is clear that the 0.99 mM BAPTA present in the internal solution is unable to adequately buffer Ca^{2+} entering through TRPC5 channels.

From six cells where TRPC5 currents and intracellular [Ca^{2+}] were simultaneously measured, five cells underwent potentiation of the current (Fig. 5 C). In those cells, the intracellular [Ca^{2+}] at 50% maximal dI/dt ranged from 611 to 1,802 nM (mean 1,117 ± 222 nM). Cells in which the 50% maximal TRPC5 current dI/dt occurred at lower [Ca^{2+}] tended to reach higher absolute dI/dt values and have shorter latencies compared with cells where the current and intracellular [Ca^{2+}] developed slowly. The variation in calcium sensitivity is visible when the current densities at −40 mV, from the initial application of CCh until the peak, are normalized to their own maximum and plotted against the recorded intracellular [Ca^{2+}] (Fig. 5 D). Despite latencies varying from 48 to 216 s in these cells, the TRPC5 current increased in a graded manner with intracellular [Ca^{2+}]. One of the five cells had a very high initial [Ca^{2+}] of ~1,500 nM and significant basal current; the 50% maximal dI/dt point occurred at 1,802 nM.

In the one cell that did not undergo potentiation, TRPC5 current activated with a single-exponential time course, and the intracellular [Ca^{2+}] reached a transient peak of 615 nM, before declining to ~360 nM over 125 s. The current in this cell also declined, displaying an unusually fast desensitization that was rarely seen in other cells.

The fura-2 imaging experiments above indicate that intracellular [Ca^{2+}] over ~600 nM enables the potentiation of TRPC5 channels; however, [Ca^{2+}] was constantly

changing in those cells. Any delays between the $[Ca^{2+}]$ elevation and channel potentiation might lead to an underestimate of the Ca^{2+} sensitivity for potentiation. To confirm that ~1 μM intracellular $[Ca^{2+}]$ causes potentiation of TRPC5 channels, we recorded CCh-activated currents from TRPC5/M1R-expressing HEK cells using internal solutions where calculated free $[Ca^{2+}]$ was buffered to levels varying from 100 nM to 17 μM. These experiments were performed in nominally Ca-free external solution to prevent escape from control of the internal Ca^{2+} buffer, as was evident in Fig. 5.

Fig. 6 A shows the CCh-activated TRPC5 current recorded from cells using a Cs-Asp internal solution with 350 nM of calculated free $[Ca^{2+}]$ buffered with 10 mM BAPTA, or with 1.8 μM of calculated free $[Ca^{2+}]$ buffered with 5 mM HEDTA. The application of 100 μM CCh in both cases activated a current during voltage ramps that had the typical TRPC5 shape: outwardly rectifying, with reversal near 0 mV and a flat region between 0 and +40 mV. The activation of the current followed a single-exponential time course and was complete within ~30 s; after this point, the current maintained its amplitude or declined slightly as the agonist application continued. However, the amplitude of the current density at −40 mV recorded with 350 nM of calculated free Ca^{2+} was −1.23 pA/pF, whereas with 1.8 μM of internal $[Ca^{2+}]$ it was >100-fold larger, at −131.8 pA/pF.

Fig. 6 B summarizes the average CCh-activated current densities at −40 mV for TRPC5/M1R-expressing cells recorded with a range of internal $[Ca^{2+}]$. The TRPC5 current amplitude has a sharp dependence on calculated free $[Ca^{2+}]$ in the internal solution and was essentially maximal when internal $[Ca^{2+}]$ was >1 μM, similar to the result from the fura-2 imaging experiments. When the pipette solution calculated free $[Ca^{2+}]$ was buffered to 100, 200, or 350 nM (all with 10 mM BAPTA), the currents at −40 mV were small, similar to the cell shown in Fig. 6 A. The average current density at −40 mV from cells recorded with internal solutions up to 350 nM of calculated free $[Ca^{2+}]$ was less than ~−2.5 pA/pF. These values are similar to the TRPC5 current amplitudes recorded using internal solutions with 100 nM of calculated free $[Ca^{2+}]$ buffered with 1 mM EGTA or BAPTA in external solutions with no added Ca (e.g., Fig. 3, trace *b*; average current density at −40 mV was −0.94 ± 0.29 pA/pF, $n = 7$, and −4.78 ± 1.04, $n = 6$, respectively). The similarity in current density amplitudes again suggests that regardless of possible direct inhibition of PLC by BAPTA, TRPC5 currents are small when calculated free $[Ca^{2+}]$ was in the range of 100 to 350 nM.

In contrast, CCh-activated TRPC5 currents recorded with internal solutions >1 μM were much larger. The average current densities at −40 mV from cells recorded using internal solutions with 1.4, 1.8, or 17 μM of calculated free $[Ca^{2+}]$ (buffered with 10 or 5 and 5 mM

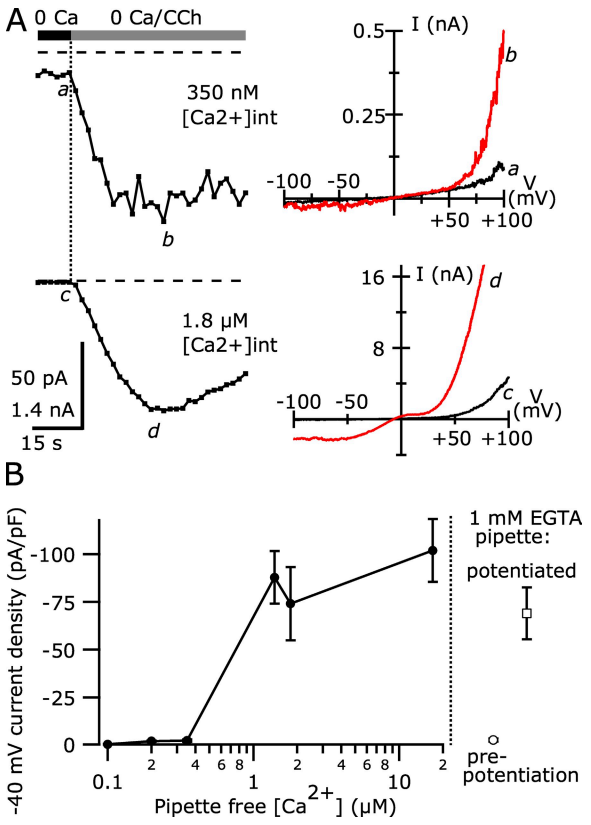

Figure 6. Internal free $[Ca^{2+}] > 1$ μM dramatically increases TRPC5 current density. (A; Left) The average CCh-activated current at −40 mV in a TRPC5/M1R-expressing cell recorded with an internal solution containing ~350 nM of calculated free $[Ca^{2+}]$ (top) and in a different cell recorded with an internal solution with ~1.8 μM of calculated free $[Ca^{2+}]$ (bottom). The currents recorded with 350 nM of calculated free $[Ca^{2+}]$ are shown on an expanded current scale. (Right) I-V curves elicited by ramp voltage stimuli before the application of 100 μM CCh (*a*) and during the peak of the response (*b*). The external solution was nominally Ca free. The currents recorded with 350 nM of calculated free internal $[Ca^{2+}]$ were digitally smoothed using a Gaussian filter (−3db = 1 kHz; top). (B) The average peak CCh-activated current density at −40 mV from cells recorded with internal solutions with varying calculated free internal $[Ca^{2+}]$. Also shown are the average current densities at −40 mV of CCh-activated TRPC5 currents in nominally Ca-free external solution before and after potentiation, recorded with 1 mM of EGTA-containing internal solutions. The average current density at −40 mV with 100 nM of calculated free $[Ca^{2+}]$ was −0.40 ± 0.08 pA/pF ($n = 8$), with 200 nM it was −2.08 ± 0.37 pA/pF ($n = 22$), and with 350 nM it was −2.44 ± 0.63 pA/pF ($n = 8$). Higher calculated free $[Ca^{2+}]$ values gave the following: 1.4 μM, −87.95 ± 13.81 pA/pF ($n = 10$); 1.8 μM: −74.13 ± 19.19 pA/pF ($n = 7$); and 17 μM: −102.03 ± 16.38 pA/pF ($n = 9$). Error bars represent ± SEM; missing error bars are smaller than symbols. Internal solutions with calculated $[Ca^{2+}] <$ 350 nM each contained (in mM): 110 Cs-Asp, 10 CsCl, 2 $MgCl_2$, 10 Cs_4-BAPTA, 4 MgATP, 0.3 Na-GTP, and 10 HEPES, pH 7.20 with CsOH, with 3.1 $CaCl_2$ for 100 nM $[Ca^{2+}]$, 4.7 mM $CaCl_2$ for 200 nM, and 6.0 mM $CaCl_2$ for 350 nM. Internal solutions with calculated free $[Ca^{2+}] > 1$ μM each contained (in mM): 150 Cs-Asp, 2 $MgCl_2$, 4 MgATP, 0.3 NaGTP, and 10 HEPES, pH 7.20 with CsOH, and the following $CaCl_2$ and HEDTA: 1.11 $CaCl_2$ and 10 HEDTA for 1.4 μM $[Ca^{2+}]$, 0.43 $CaCl_2$ and 5 HEDTA for 1.8 μM $[Ca^{2+}]$, and 1.89 $CaCl_2$ and 5 HEDTA for 17 μM $[Ca^{2+}]$.

HEDTA, respectively) ranged from ~−74 to −102 pA/pF. These values are only slightly larger than the average current density at −40 mV reached in cells recorded with 100 nM of calculated free [Ca^{2+}]/1 mM BAPTA internal solutions immediately after the return to nominally Ca-free external solution from the potentiated amplitude (e.g., Fig. 3 C, trace *e*), which was −69.04 ± 13.69 pA/pF (n = 8). This suggests that TRPC5 channels recorded using high [Ca^{2+}] internal solutions in nominally Ca-free external solution might be in the same potentiated state as that reached by most cells recorded using 1 mM EGTA- or BAPTA-buffered internal solutions and normal 2 Ca external solution.

TRPC5 channels potentiated by internal Ca^{2+} do not increase their permeability to large cations

The biphasic agonist activation resulting in large amplitude and more linear inward TRPC5 currents bears some resemblance to the large enhancement of TRPV1- and TRPV3-mediated currents during strong agonist stimulation (Chung et al., 2005; Chung et al., 2008). In these channels, prolonged activation with high concentrations of agonist reportedly can lead to an increase in the permeability to large cations such as NMDG. To directly assess whether TRPC5 channels change their permeability properties during potentiation by intracellular Ca^{2+}, we monitored the reversal potential of the CCh-activated current when extracellular Na^+ was completely replaced by NMDG (Fig. 7). 100 µM CCh was initially applied to TRPC5/M1R-expressing cells in a nominally Ca-free external solution with NMDG; the absence of external Ca^{2+} prevented the potentiation of TRPC5 current. Then, the external solution was changed to 2 Ca external solution, with 150 mM NaCl and 2 mM $CaCl_2$. This allowed Ca^{2+} to enter and caused subsequent potentiation of TRPC5 channels. For the cell shown in Fig. 7 A, the very large peak current at −100 mV of −11.6 nA indicates that the channels were very likely potentiated. Next, the external solution was replaced with one containing NMDG, still with 2 mM $CaCl_2$ present to maintain high intracellular [Ca^{2+}] and current potentiation. Finally, we removed Ca^{2+} from the external NMDG solution and monitored the reversal potential soon after external Ca^{2+} removal, when TRPC5 channels were still potentiated, and ~60 s later, when potentiation was almost fully reversed. In both cases the external solution was identical, so that any change in the reversal potential would result from alterations in active conductances or their properties.

The current–voltage curves of CCh-activated TRPC5 channels recorded in nominally Ca-free NMDG external solutions are shown in Fig. 7 B. Inward currents at −100 mV were small, only 1.5–2.5% of the level in normal Ca^{2+}- and Na^+-containing external solution, reflecting the poor absolute permeability of $NMDG^+$. The reversal potential of these currents was −65 mV. At voltages depolarized from the reversal potential, the outward current carried by Cs^+ increased, until it began to decline as V_m reached 0 to +25 mV. This reduction is presumably the result of increasing block by internal Mg^{2+}, which is responsible for the flat portion of the I-V in normal external sodium (Obukhov and Nowycky, 2005). Positive to ~+25 mV, the current was strongly outwardly rectifying. As the potentiation of TRPC5 channels declined, there was a minimal shift in the reversal potential even as the current at −100 mV decreased from ~−250 to ~−12 pA. This demonstrates that although TRPC5 is somewhat permeable to NMDG, its permeation does not change with intracellular Ca^{2+} potentiation. From two cells, the reversal potential of

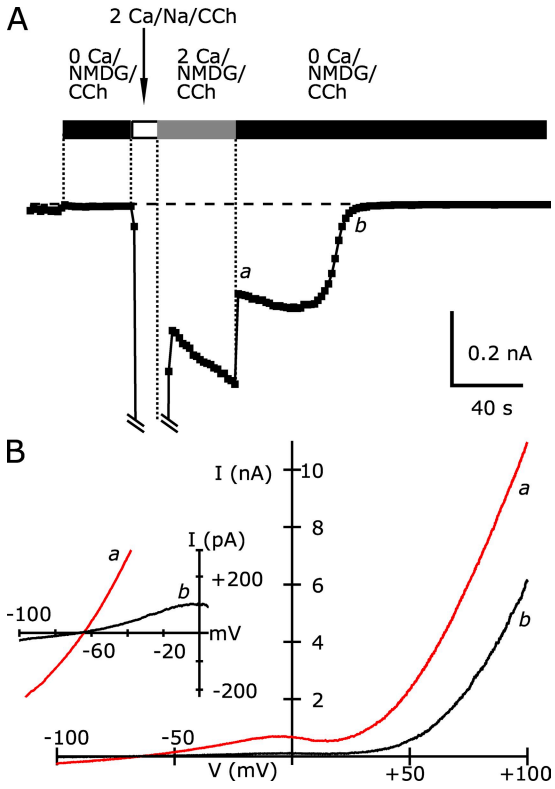

Figure 7. Potentiation by intracellular Ca^{2+} does not alter NMDG permeability of TRPC5. (A) The average −100-mV current preceding voltage ramps in response to the application of the indicated external solutions (5 ms at −100 mV immediately before the ramp was averaged in this case). Black bars indicate the addition of nominally Ca-free NMDG external, the open bar indicates the application of 2 Ca external solution, and the gray bar indicates the application of 2 Ca and NMDG external (100 µM CCh present throughout). (B) I-V relation of currents elicited by 200-ms voltage ramps recorded with nominally Ca-free NMDG/CCh external solution ~2 s after the removal of external Ca^{2+} (*a*) and 64 s later (*b*). (Inset) The region near the reversal potential on an expanded scale. To emphasize the reversal potential, traces were digitally smoothed using a Gaussian filter (−3db = 500 Hz). Internal solution (in mM): 150 Cs-Asp, 2 $MgCl_2$, 0.36 $CaCl_2$, 1 EGTA, 4 MgATP, 0.3 NaGTP, and 10 HEPES, pH 7.20 with CsOH. External NMDG solutions (in mM): 150 mM NMDG-Cl, 4 KCl, 10 glucose, 10 HEPES, pH 7.40, with HCl, and 2 $CaCl_2$ with 1 $MgCl_2$ or 3 mM $MgCl_2$ alone.

TRPC5 current in NMDG external solutions immediately after the removal of external Ca^{2+} was ~3 mV more depolarized than after the potentiation declined. This value is much smaller than the >40-mV depolarizing shift demonstrated in NMDG external solutions for either TRPV1 channels (Chung et al., 2008) or TRPV3 channels (Chung et al., 2005).

Intracellular Ca^{2+} also potentiates agonist-activated TRPC4 channels

TRPC5 and TRPC4 are closely related, sharing 80% sequence similarity. They also share many of the same functional characteristics, including activation by Gαq/11-coupled receptors and potentiation by external Ca^{2+} and lanthanides (Schaefer et al., 2000, 2002; Strubing et al., 2001). We tested whether intracellular Ca^{2+} can potentiate TRPC4 channels as well as TRPC5 channels. In HEK cells expressing the TRPC4β isoform and M1Rs, the application of 100 µM CCh activated a current with a similar I-V relation to TRPC5 (Fig. 8 B). We used this isoform as it tends to result in larger currents compared with TRPC4α. Despite the use of internal solutions with 100 nM of calculated free [Ca^{2+}] and 1 mM EGTA, we never observed biphasic activation in any of the 10 cells recorded for up to 60 s in CCh. Instead, the current activated with a single-exponential time course and remained at steady state throughout the CCh application (Fig. 8 A). The average TRPC4β-mediated currents were small, −8.35 ± 2.9 pA/pF at −40 mV ($n = 10$), similar in amplitude to TRPC5-expressing cells that did not undergo potentiation (e.g., Fig. 1 C). One cell did have a peak current density at −40 mV of −30.0 pA/pF, but its activation was not biphasic.

Because the addition of 10 Ca external solution potentiated TRPC5 current in 13 of 15 cells (Fig. 4), we tested whether high external Ca^{2+} would also potentiate TRPC4 current (Fig. 8 B). TRPC4β current was activated by the application of 100 µM CCh for 20–30 s, until a new steady state was reached. When the external solution was changed to 10 Ca external solution, only one of three cells underwent an increase in current amplitude at −40 mV. The current peaked after 6 s at an amplitude 2.9-fold larger than in the standard 2 Ca external solution. This is much smaller than the ~14-fold increase we found for TRPC5 channels. After the peak, the current began to decline rapidly, such that after 64 s the current was reduced by 65%.

The small inward current amplitudes recorded from TRPC4β/M1R-expressing cells might have resulted in only modest intracellular [Ca^{2+}] increases, despite raising external Ca^{2+} to 10 mM. Thus, we tested whether supplying elevated [Ca^{2+}] in the internal solution could lead to large amplitude TRPC4β currents. As in similar experiments with TRPC5 channels (Fig. 6), we recorded these currents in external solutions with nominally Ca-free external solution, preventing Ca^{2+} entry

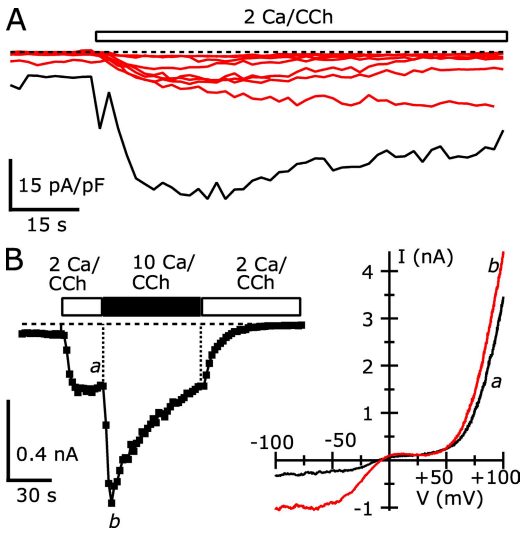

Figure 8. Heterologously expressed TRPC4β channels are potentiated by intracellular Ca^{2+}. (A) TRPC4β current densities at −40 mV during the application of 100 µM CCh recorded from nine cells. One cell, with ~−30 pA/pF current density, is shown in black; the remaining currents were less than −17 pA/pF and are shown in red. (B; Left) The application of 10 Ca external solution–potentiated TRPC4β channels. The average −40-mV current from a TRPC4β-expressing cell (not shown in A) in response to 100 µM CCh in standard 2 Ca external (open bar) or 10 Ca external (black bar). (Right) I-V relation of current elicited by voltage ramps applied at the times is indicated by lowercase letters. Internal solution contained (in mM): 150 Cs-Asp, 2 $MgCl_2$, 0.36 $CaCl_2$, 1 EGTA, 4 MgATP, 0.3 NaGTP, and 10 HEPES, pH 7.20. External solutions both contained 1 mM $MgCl_2$.

(not depicted). The average current density at −40 mV recorded from three TRPC4β/M1R-expressing cells using the internal solution with 1.8 µM [Ca^{2+}] and 5 mM HEDTA was −32.6 ± 7.7 pA/pF. Thus, average currents were enhanced approximately fourfold relative to currents recorded with low Ca^{2+} buffering (despite the absence of Ca^{2+} in the external solution), suggesting that intracellular Ca^{2+} also potentiates TRPC4β channels. The inability of 10 mM of external Ca^{2+} to potentiate currents and the smaller average current densities with elevated [Ca^{2+}] in the internal might result from lower expression of TRPC4β channels or from the apparently enhanced desensitization of TRPC4 compared with TRPC5 (Schaefer et al., 2000). We did not test other isoforms of TRPC4; whether they might differ in potentiation by Ca^{2+} is unknown.

TRPC5 channel potentiation by intracellular Ca^{2+} results from an increase in open probability

In principle, the intracellular Ca^{2+}-dependent potentiation of TRPC5 channels could result from increases in the number of active channels, in the single-channel conductance, or in the channel open probability. The different extent and kinetics of inward current potentiation relative to outward current suggest that increases in the number of active channels alone cannot underlie

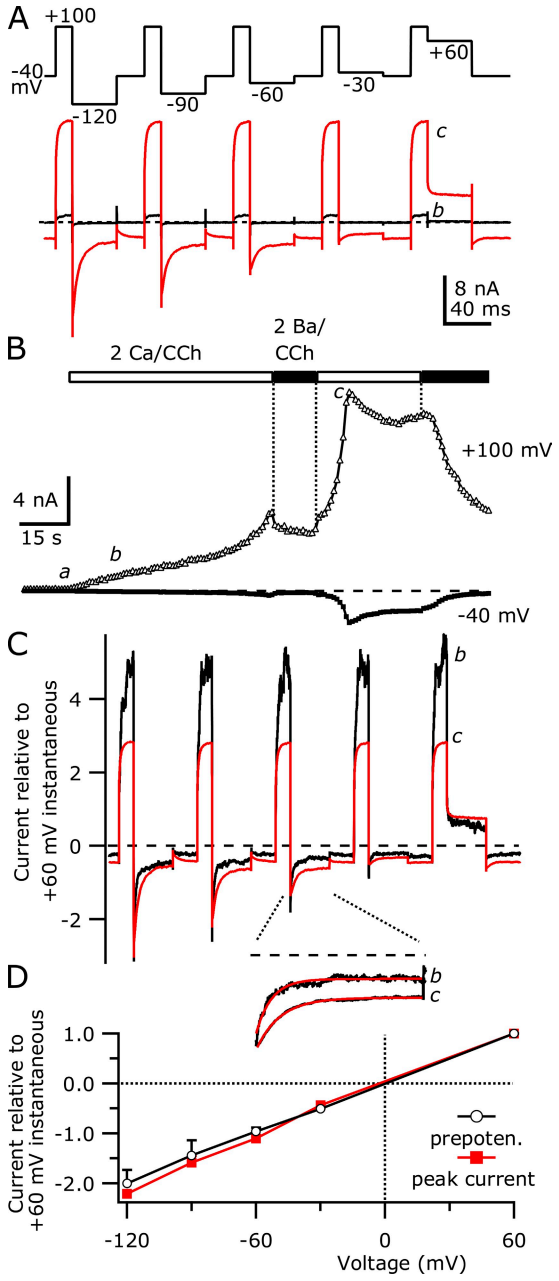

Figure 9. The TRPC5 open channel I-V relationship does not change during intracellular calcium potentiation. (A) CCh-activated TRPC5 currents were elicited by 15-ms voltage steps to +100 mV, followed by 40-ms steps to multiple hyperpolarizing potentials (applied at 1 Hz). The black trace shows the current recorded ~15 s after the addition of 100 μM CCh, and the red line shows the peak currents recorded 91 s after CCh addition (lowercase letters indicate sweep timing in B). (B) The average CCh-activated TRPC5 currents at +100 mV (triangles, final 3 ms of first +100-mV conditioning pulse) and −40 mV (squares, 10-ms average at sweep onset) during the application of 2 Ca external (open bars) and 2 Ba external solution (black bar). *a*, the timing of sweeps used for subtraction of the uncompensated capacity current. (C) Capacity-corrected traces from A were normalized to the amplitude of the TRPC5-mediated current 0.7 ms after repolarization to +60 mV to account for the large difference in absolute current amplitudes. The smaller relative +100-mV current in *c* likely indicates that the open probability at +60 and +100 mV are more similar after potentiation. The resulting instantaneous tail currents were similar. (Inset) The tail current at −60 mV on an expanded scale. The solid red lines show single-exponential fits to the current. (D) The size of the CCh-activated TRPC5 tail currents after normalization (as in C) was measured in three to six cells both before (black open circles, ~30 or fewer seconds after CCh addition) and after (red squares, 100 s or fewer after CCh, when current reached peak amplitude) potentiation. Currents were measured 0.7–0.85 ms after the +100-mV conditioning pulse to allow any uncorrected fast capacity current to settle. Error bars show SEM; absent error bars are smaller than symbol. Internal solution (in mM): 150 Cs-Asp, 2 $MgCl_2$, 0.36 $CaCl_2$, 1 EGTA, 4 MgATP, 0.3 NaGTP, and 10 HEPES, pH 7.20 with CsOH (100 nM calculated free [Ca^{2+}]). External solution: 2 Ca external and 2 Ba external ($CaCl_2$ completely replaced by $BaCl_2$; all else the same).

calcium potentiation. We tested whether the conductance of TRPC5 channels changed by measuring the open-channel I-V relation before and after potentiation by intracellular Ca^{2+}. CCh-activated TRPC5 currents were recorded using pipette solutions with low calcium buffering in the presence of standard 2 Ca external solution. To measure the open-channel I-V, 15 (or 50)-ms conditioning pulses were applied to activate TRPC5 channels, and the tail currents immediately after hyperpolarization to a range of potentials were recorded. Fig. 9 A shows the voltage-dependent activation and deactivation of TRPC5 channels 15 and 91 s after the application of 100 μM CCh. Currents were initially small in amplitude (+1.19 nA at +100 mV), presumably before intracellular Ca^{2+} potentiation. The current continued increasing, interrupted only by the replacement of external calcium with barium, which prevented the current increase similar to magnesium replacement (Fig. 9 B, c.f., Fig. 3). After external calcium was reapplied, the TRPC5 current rapidly increased as calcium potentiation occurred, reaching a peak amplitude of +17.45 nA. Furthermore, large inward tail currents were visible in response to the hyperpolarizing steps. Note that the current amplitudes at +100 mV were constant throughout the sweep; under these conditions, there is little or no use dependence of TRPC5 channels during repetitive depolarizations.

To compare the open-channel I-V before and after potentiation, when current amplitudes varied up to a factor of 10, we normalized the currents to the amplitude of the current immediately after the repolarization to +60 mV (Fig. 9 C). We measured the relative instantaneous tail current during the hyperpolarizing potentials at the same time point where the TRPC5 channel open probability, reached during the +100-mV conditioning pulse (or +90 mV for some cells), remains constant. We used the smaller current amplitudes at +60 mV for normalization rather than the +100-mV amplitude to minimize possible effects of uncompensated series resistance when currents at +100 mV were very large. From six cells we found that the instantaneous I-V relationship was

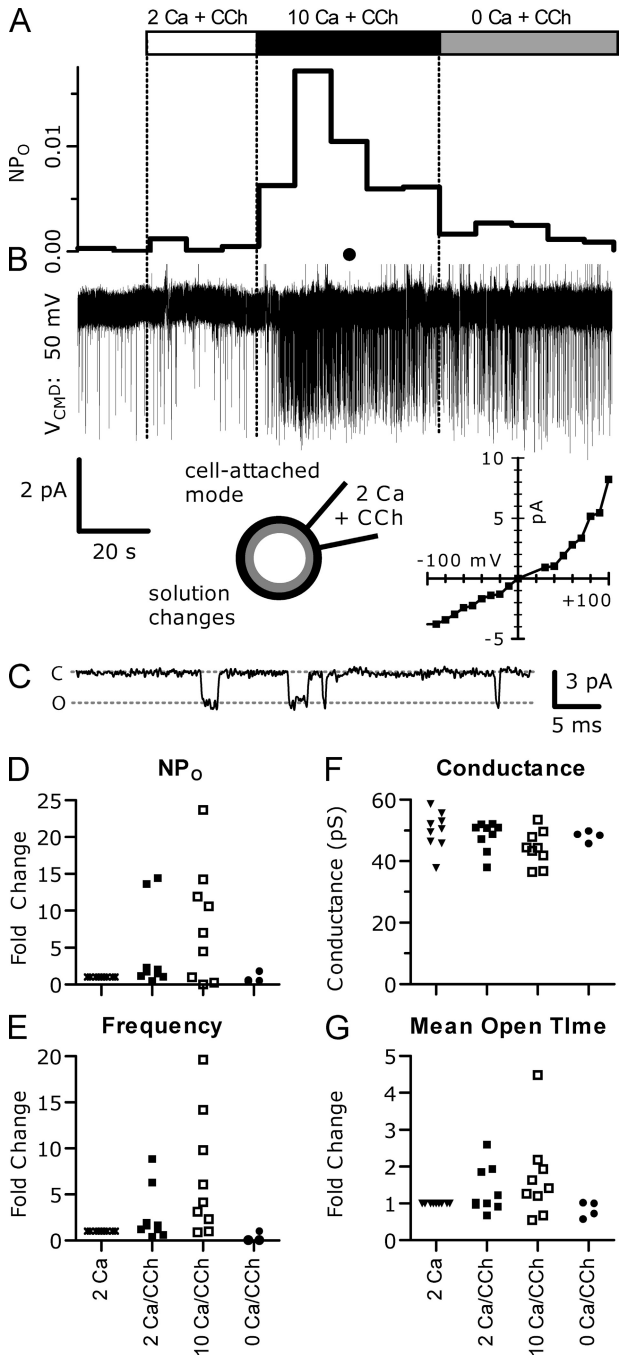

Figure 10. Potentiation of a single TRPC5 channel by Ca^{2+} in cell-attached recordings. (A) Channel activity as shown by continuous NP_o trace (averaged 10-s bins). (B) The current trace recorded −50 mV relative to the cell membrane potential. Channel openings are downward deflections from the baseline. (Bottom right) Single-channel I-V relation. (C) Expanded trace for the region indicated by the black circle in B. C and O indicate closed and open levels, respectively. (D–G) Summary of single-channel properties from nine independent patches (normalized as fold change relative to preceding condition due to baseline NP_o variability from patch to patch). The large increase in single-channel activity (NP_o) evoked by the addition of 10 mM of extracellular Ca^{2+} in D (10.42 ± 2.8-fold; n = 7; P = 0.025), resulted from (E) increased channel-opening frequency (9.76 ± 2.13-fold; n = 8; P = 0.003) and (G) channel open time (2.09 ± 0.38-fold; n = 8; P = 0.011). (F) Single-channel conductance did not change. In this figure and Fig. 11, symbols represent patches recorded in the bath solutions indicated; for clarity, patches at similar amplitudes are offset horizontally and shown in different shapes for different solution conditions. Internal solution: standard 2 Ca external with 100 μM CCh. Bath solutions: 2 Ca and 10 Ca each had 1 mM $MgCl_2$. Nominally Ca-free external had 3 mM $MgCl_2$.

not affected by intracellular Ca^{2+} potentiation (Fig. 9 D). For example, the relative peak tail current at −60 mV was −0.967 ± 0.076 before potentiation and −1.107 ± 0.058 after potentiation. The larger inward currents after potentiation were instead caused by a slower and less complete deactivation of the tail current. Tail currents at −60 mV before intracellular Ca^{2+} potentiation deactivated with a single exponential with a tau of 2.54 ± 0.44 ms, which increased to 3.91 ± 0.54 ms after potentiation. Thus, the fivefold difference in potentiation between inward and outward TRPC5 currents is not likely to arise from large, asymmetrical changes in channel conductance.

To gain further understanding of the biophysical changes that occur during potentiation of TRPC5 by intracellular Ca^{2+}, we performed cell-attached recordings from TRPC5/M1R-expressing HEK cells using pipettes filled with the standard 2 Ca external solution and 100 μM CCh (Fig. 10, A–C). Cells were initially bathed in 2 Ca external solution, and TRPC5 channel activity at −50 mV was recorded for ∼20 s. Despite the presence of CCh in the pipette, TRPC5 activity remained low. At this point, 100 μM CCh in 2 Ca external solution was added to the bath, activating M1R receptors and TRPC5 channels throughout the cell. In two of nine cells, this led to a dramatic increase in NP_o (number of channels multiplied by the open probability) of 14.0 ± 0.39-fold (P = 0.017), with a 14.3–17.1-s delay. Because in these experiments it is unknown whether intracellular [Ca^{2+}] reached levels sufficient to cause potentiation, we then added 10 Ca external solution with CCh to the bath to increase Ca^{2+} entry, similar to whole cell experiments shown in Fig. 4. In the two cells that already displayed an elevated NP_o, the addition of 10 Ca external solution with CCh caused no further change. In six of the remaining seven cells tested, perfusion of 10 Ca external solution and CCh caused a dramatic increase in NP_o: the average peak increase in NP_o was ∼10-fold, with a delay <10 s. To test whether this increase in TRPC5 channel NP_o was due to the increase in intracellular [Ca^{2+}], we changed the bath solution to nominally Ca free with CCh in four patches (Fig. 10 D). This led to a large decrease in NP_o that reached levels similar to initial 2 Ca external solution alone (0.86 ± 0.32-fold; P = 0.16). The lower peak potentiation of NP_o in these experiments compared with whole cell experiments might result from lower [Ca^{2+}] caused by a reduced driving force on Ca^{2+} in the cell-attached configuration. The activation of large TRPC5 currents after bath CCh addition would likely drive cells

to ~0 mV, compared with the −40-mV holding potential used in whole cell recordings.

The increase in NP_o was apparently derived from a substantial increase in the frequency of channel openings (Fig. 10 E): the average increase during Ca^{2+} potentiation was approximately ninefold, whereas 0 Ca^{2+} and CCh perfusion returned frequency to near initial levels. Channel mean open time also increased (Fig. 10 G) on average approximately twofold, which reversed upon perfusion of nominally Ca-free external solution (1.1 ± 0.2; P = 0.34). Concurrently, channel mean closed time decreased substantially: before potentiation closed time was 64.6 ±4.5 ms (n = 697 closings), but during potentiation it dropped to 15.4 ± 0.2 ms (n = 751 closings; P < 0.0001).

It is unclear whether the changes in NP_o were the result of an increase in the number of active channels in the patch or an increase in single-channel open probability. Three patches contained occasional double openings that could be observed under all conditions, indicating the presence of multiple channels. However, we never observed an increase in the number of open channel levels during Ca^{2+} potentiation of TRPC5, although in some cases NP_o was quite low (ranging from 0.003 to 0.376). The NP_o of patches with one apparent channel is similar to previous reports (Schaefer et al., 2000; Jung et al., 2003; Obukhov and Nowycky, 2008). For those patches in which only one channel was observed even after Ca^{2+} potentiation (average NP_o was 0.0562 ± 0.034, range 0.0033–0.156; n = 5), we used the following equation to estimate the probability that the observed openings during Ca^{2+} potentiation were actually the result of two channels (Colquhoun and Hawkes, 1995): $P(r > n_O) = \mu^{(n_o - 1)}$, where $\mu = (1-P_o)/(1-P_o/2)$, and n_O = observed number of single-channel openings (in our case, n_O = 1,562). By this calculation, the maximum probability of more than one channel being present during Ca^{2+} potentiation in those patches was $\sim 10^{-20}$. Therefore, we suggest that the primary effects of Ca^{2+} potentiation are to increase open probability via a small increase in mean open time and a larger decrease in closed time.

We found that the single-channel conductance was unchanged during Ca^{2+} potentiation of TRPC5 (Fig. 10 F). Before Ca^{2+} potentiation, the average single-channel conductance was 50.36 ± 4.1 pS, whereas after potentiation it was 49.65 ± 4.7 pS (after 0 Ca^{2+} and CCh perfusion it was 53.19 ± 5.1 pS). The single-channel conductance of TRPC5 at negative membrane potentials is reportedly 38–48 pS (Schaefer et al., 2000; Yamada et al., 2000; Strubing et al., 2001). The slightly larger conductance that we observed might result from an added contribution of the cell's resting potential. The single-channel current–voltage relation (Fig. 10 B) was outwardly rectifying, closely resembling previous reports (Jung et al., 2003; Obukhov and Nowycky, 2008).

These data support the hypothesis that Ca^{2+} entry through a single TRPC5 channel does not cause maximal potentiation of that channel. 100 µM CCh was included in the pipette so that TRPC5 channels within the patch were likely to be activated and passing Ca^{2+} for ~30 s before bath perfusion of CCh. If the resulting Ca^{2+} elevation near the activated TRPC5 channels in the patch saturated the potentiation mechanism, increases in bulk Ca^{2+} after the addition of CCh and 2 or 10 mM Ca^{2+} to the bath would not induce further potentiation. Instead, the ~10-fold potentiation of NP_o we observed after the bath addition of CCh and Ca^{2+} suggests that Ca^{2+} that has flowed into the cell through other TRPC5 channels is also sensed by the TRPC5 recorded in the patch.

To directly determine the effect of varying [Ca^{2+}] at the cytosolic face of TRPC5 channels, we performed excised inside-out patch recordings from TRPC5 and M1R-transfected HEK cells, again with 2 Ca external solution and 100 µM CCh in the pipette. The cytosolic face of the patch was exposed to solutions of varying calculated free [Ca^{2+}] to determine whether TRPC5 channels were intrinsically sensitive to Ca^{2+}. In 5 of 12 patches, we observed a dramatic potentiation of single-channel activity when the intracellular surface of the channel was exposed to 1.8 and 100 µM Ca^{2+}, with NP_o increasing ~23-fold and 45-fold over 100 nM Ca^{2+}, respectively (Fig. 11, A–E). One of these responsive patches was dramatically stimulated by Ca^{2+} with NP_o increasing ~150-fold in 100 µM Ca^{2+}. Latency to peak activity ranged from <2 to 20 s. Single-channel conductance ranged from 45 to 49 pS and did not systematically change with bath solution. Similar to the cell-attached recordings, the increase in NP_o was due to a large increase in the number of channel openings and increased mean open time. Compared with 0.1 µM of calculated free Ca^{2+}, the frequency of openings in 1.8 µM of calculated free Ca^{2+} increased by ~15-fold, and in 100 µM Ca^{2+} by ~34-fold. The stimulation of channel activity was also caused by an increase in mean open time, which was ~50% for both 1.8 µM of calculated free Ca^{2+} and in 100 µM Ca^{2+}. Returning patches to low [Ca^{2+}] caused the channel activity to decrease, indicating that the potentiation was reversible, as in whole cell recordings.

The remaining seven patches were not responsive to changes in [Ca^{2+}] (Fig. 11 F). Most of these patches initially displayed a relatively high NP_o, even in 0.1 µM of calculated [Ca^{2+}], but open times and conductance were similar to the other five patches. These patches might contain channels that are already potentiated and locked in this state. Collectively, these results suggest that in some cases the ability of Ca^{2+} to strongly increase TRPC5 channel activity can survive patch excision, and that this potentiation might reflect the same processes that occur during the potentiation seen in whole cell experiments. However, the absence of potentiation in some patches suggests that an important factor was lost upon patch excision.

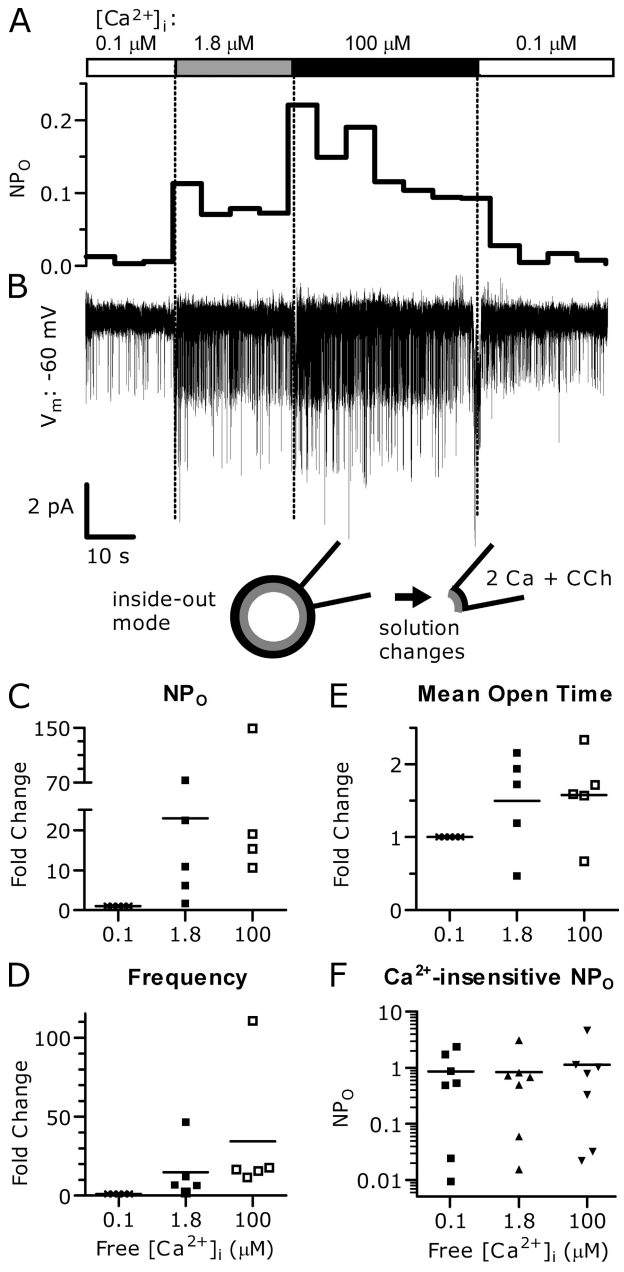

Figure 11. TRPC5 channel activity is potentiated by increases in $[Ca^{2+}]$ in excised (inside-out) single-channel recordings. The cytosolic face of TRPC5 channels was exposed to varying $[Ca^{2+}]$ using excised patches from TRPC5 and M1R cotransfected HEK cells. (A) Channel activity NP_o trace from a single patch in response to changing Ca^{2+} (NP_o was averaged over 5-s bins). (B) Current recorded at −60 mV; channel openings are downward deflections from the baseline. (C) Stimulation of peak NP_o from five patches with containing TRPC5 channels (relative to 100 nM Ca^{2+}, NPo in 1.8 μM of calculated Ca^{2+}: 22.9 ± 13.1-fold [median 10.9; P = 0.043; *t* test]; in 100 μM Ca^{2+}: 45.1 ± 26.27-fold [median 18.99; P = 0.048]). (D) Elevated cytosolic Ca^{2+} increases the frequency of channel openings. Fold increases were 14.81 ± 8.09 (median 6.89; $n = 4$; P = 0.032) in 1.8 μM Ca^{2+} and 34.42 ± 19.07 (median 16.57; $n = 4$; P < 0.0001) in 100 μM Ca^{2+}. (E) Elevated cytosolic Ca^{2+} increased TRPC5 channel mean open time. Fold increase in mean open time was 1.5 ± 0.3-fold in 1.8 μM Ca^{2+} ($n = 5$; P = 0.01) and 1.58 ± 0.27-fold in 100 μM Ca^{2+} ($n = 5$; P = 0.001). (F) In seven additional patches, elevated Ca^{2+} did not increase NP_o; these typically had high initial NP_o. Internal solution: 2 Ca external with 100 μM CCh. Bath solutions: 0.1 μM of calculated free $[Ca^{2+}]$ solution (in mM): 150 Cs-Asp, 2 $MgCl_2$, 0.36 $CaCl_2$, 1 EGTA, 4 MgATP, 0.3 NaGTP, and 10 HEPES, pH 7.20 with CsOH. 1.4 μM of calculated free $[Ca^{2+}]$ solution (in mM): 150 Cs-Asp, 1.11 $CaCl_2$, 10 HEDTA, 2 $MgCl_2$, 4 MgATP, 0.3 NaGTP, and 10 HEPES, pH 7.20 with CsOH. 100 μM of free $[Ca^{2+}]$ solution (in mM): 150 Cs-Asp, 0.10 $CaCl_2$, 2 $MgCl_2$, 4 MgATP, 0.3 Na-GTP, and 10 HEPES, pH 7.20 with CsOH.

Intracellular Ca^{2+} potentiation of TRPC5 channels reduces potentiation by external Ca^{2+} and lanthanides

The results in Figs. 10 and 11 suggest that intracellular $[Ca^{2+}]$ can increase the open probability of TRPC5 at voltages ∼−50 mV, and our whole cell experiments suggest that the extent of this potentiation is voltage dependent, increasing with hyperpolarization. Potentiation of TRPC5 channels by external Ca^{2+} and lanthanides also enhances channel open probability, which increases with hyperpolarization (Jung et al., 2003). If both mechanisms exist, the ability of external Ca^{2+}/lanthanides to further increase current might be reduced when channels are already potentiated by elevated intracellular $[Ca^{2+}]$. The experiments in Fig. 3 suggest that this is the case. TRPC5 channels initially activated in nominally Ca-free external solution were not potentiated, and when 2 Ca external solution was added, the immediate increase in current presumably resulted from binding at the external Ca^{2+}/lanthanide site. On average, the current at −40 mV increased 7.02 ± 1.40-fold, whereas the current at +100 mV increased 1.61 ± 1.17-fold ($n = 8$; compare traces *b* and *c* in Fig. 3). After the addition of external Ca^{2+} led to potentiation of the TRPC5 current, intracellular $[Ca^{2+}]$ presumably reached high levels. At this point the removal of external Ca^{2+} resulted in an immediate decrease in current amplitude, reflecting loss of the potentiation at the Ca^{2+}/lanthanide site (compare traces *d* and *e* in Fig. 3). The average potentiation by 2 mM Ca^{2+} at this point was 2.22 ± 0.17-fold at −40 mV and 1.11 ± 0.04-fold at +100 mV ($n = 8$). Thus, after TRPC5 channels were potentiated by intracellular $[Ca^{2+}]$, the effect of extracellular Ca^{2+} was reduced by 68% at −40 mV and ∼31% at +100 mV.

We tested the proposed interaction between internal Ca^{2+} and external Ca^{2+}/lanthanide potentiation using internal solutions with low (200 nM) or high (1.4–17 μM) calculated $[Ca^{2+}]$ to keep TRPC5 channels in nonpotentiated and potentiated states, respectively. Using these internal solutions, we measured the response as external Ca^{2+} was increased from 0 to 10 mM (Fig. 12). TRPC5 channels were initially activated by the addition of 100 μM CCh in nominally Ca-free external solutions. After 45–60 s in CCh, the current had reached steady state and external $[Ca^{2+}]$ was increased to 0.3, 1, 3, and 10 mM. The effect of changing external Ca^{2+} on TRPC5

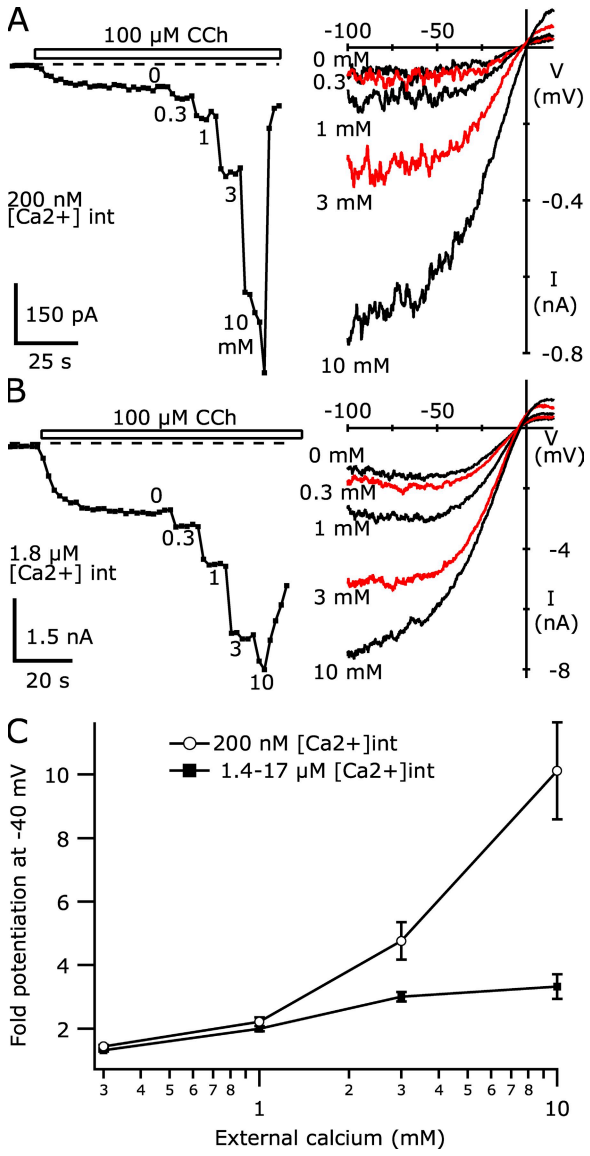

Figure 12. The extent of TRPC5 current potentiation by intracellular Ca^{2+} affects external Ca^{2+} current enhancement. (A) The average current at −40 mV recorded in a TRPC5/M1R-expressing HEK cell (left); internal solution with 200 nM of calculated free [Ca^{2+}] containing (in mM): 110 Cs-Asp, 10 CsCl, 2 $MgCl_2$, 4.7 $CaCl_2$, 10 Cs_4-BAPTA, 4 MgATP, and 0.3 NaGTP, pH 7.20 with CsOH. The right panels here and in B show the I-V curves from each initial sweep in different [Ca^{2+}]. Currents recorded in 0.3 and 3 mM of external Ca^{2+} are shown in red; all others are shown in black. (B) The average current at −40 mV using an internal solution with 1.8 μM of calculated free [Ca^{2+}] containing (in mM): 150 Cs-Asp, 2 $MgCl_2$, 0.46 $CaCl_2$, 5 HEDTA, 4 MgATP, and 0.3 NaGTP, pH 7.20 with CsOH. (C) Potentiation of current at −40 mV relative to that in nominally Ca-free external solution is plotted versus external [Ca^{2+}] for cells recorded in 200 nM of internal calculated free [Ca^{2+}] (open circles) or 1.4–17 μM of calculated free [Ca^{2+}] (filled squares). Potentiation for the 200 nM Ca internal was 1.44 ± 0.05-fold for 0.3 Ca, 2.22 ± 0.14-fold for 1 Ca, 4.77 ± 0.59 for 3 Ca, and 10.11 ± 1.53 for 10 Ca (n = 6 each); whereas, for the >1.4 μM [Ca^{2+}] internals it was 1.32 ± 0.04-fold, 2.00 ± 0.08, 3.09 ± 0.15, and 3.33 ± 0.39 (n = 10; n = 8 for 10 Ca external). External solutions had the following added divalents (in mM): 0 added $CaCl_2$ with 3 $MgCl_2$, 0.3 $CaCl_2$ with 3 $MgCl_2$, 1 $CaCl_2$ with 2 $MgCl_2$, 3 $CaCl_2$ with 1 $MgCl_2$, and 10 $CaCl_2$ with 1 $MgCl_2$.

current was immediate and remained constant during each 10-s [Ca^{2+}] application. In some cells recorded with low internal [Ca^{2+}] (Fig. 12 A), the application of 10 mM Ca^{2+} first led to an immediate increase in current that then further developed, presumably as Ca^{2+} entry escaped control of BAPTA in the internal solution. In contrast, for some cells recorded with high internal [Ca^{2+}] (Fig. 12 B), the application of 10 Ca external initially increased current (presumably as the potentiation at the external site increased), followed by a decline (as the current desensitized). For all cells, the current was averaged from the sweep immediately after the application of 10 Ca external solution exchange to minimize any contribution of these changes.

These experiments demonstrate that when TRPC5 channels were recorded with low internal [Ca^{2+}], the ability of extracellular Ca^{2+} to potentiate the current was much greater than when internal solutions with high [Ca^{2+}] were used. For internal solutions with 200 nM of calculated free internal [Ca^{2+}], the TRPC5 current densities at −40 mV increased by ∼10-fold in 10 Ca external solution (relative to the current in nominally Ca-free external). For internal solutions with 1.4, 1.8, or 17 μM of free [Ca^{2+}], we averaged the results from all cells because the potentiation by external Ca^{2+} was equal for each. Current densities at −40 mV were potentiated by only approximately threefold in the 10 Ca external solution. Overall, potentiation of TRPC5 channels was equivalent for the two sets of internal solutions at 0.3 and 1 Ca external solution. However, potentiation with high calculated free [Ca^{2+}] internals was 35% smaller for 3 Ca external solution and 67% smaller for 10 Ca external solution.

We also tested whether potentiation by La^{3+} was reduced when TRPC5 channels were potentiated by elevated intracellular [Ca^{2+}] (Fig. 13). We applied 100 μM La^{3+} during whole cell recordings of CCh-activated TRPC5 currents using internal solutions containing 200 nM, 1.8 μM, and 100 μM Ca^{2+} (to avoid competition between Ca^{2+} and La^{3+} for the external binding site, these experiments were performed in nominally Ca-free external solution). After TRPC5 currents reached steady state after CCh application, the addition of 100 μM La^{3+} potentiated TRPC5 current by ∼14.5-fold at −40 mV and ∼5.5-fold at +100 mV (200 nM of calculated free [Ca^{2+}] internal). This potentiation is larger than that caused by 3 or 10 Ca external solution (Fig. 12), as expected given the fact that La^{3+} potentiates TRPC5 current in the presence of 2 mM of external Ca^{2+} (Jung et al., 2003).

At higher internal [Ca^{2+}], we observed a voltage-dependent reduction in La^{3+} potentiation. With 1.8 μM of calculated internal [Ca^{2+}], 100 μM $LaCl_3$ potentiated

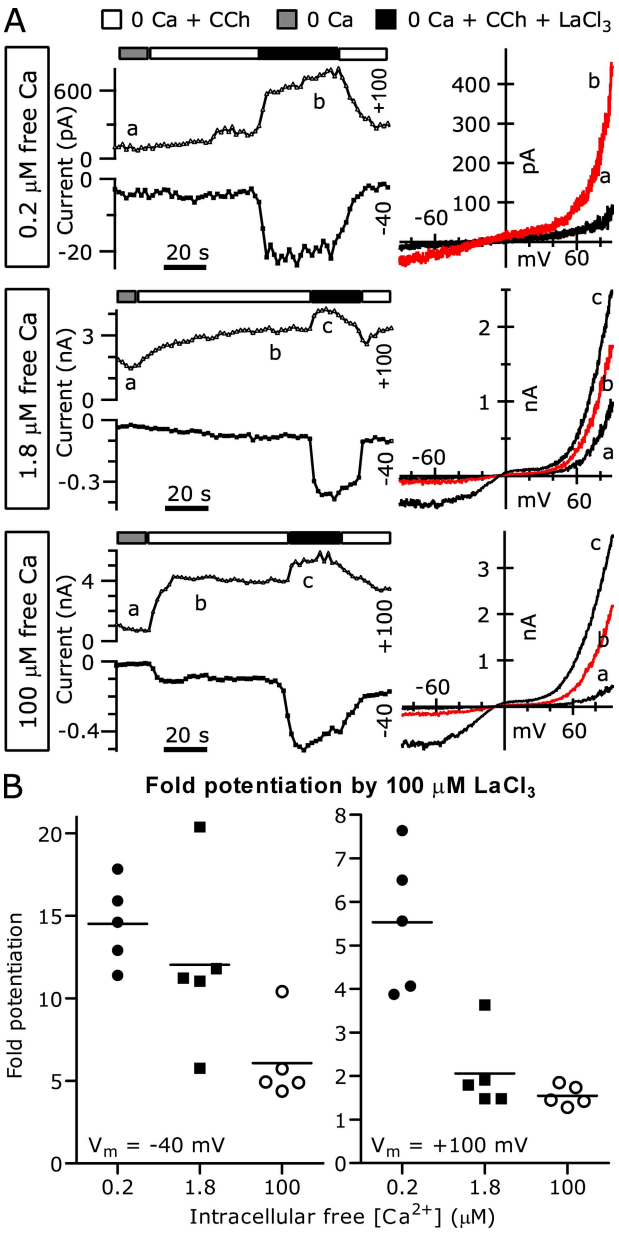

Figure 13. Increased internal [Ca^{2+}] depresses TRPC5 current potentiation by La^{3+}. (A; Left) The average currents at +100 mV (triangles) and −40 mV (squares) recorded from TRPC5 and M1R cotransfected HEK cells during voltage ramps applied in the indicated solutions. (Right) I-V relations from the times indicated by lowercase letters. Boxes to the left of each trace indicate the calculated free [Ca^{2+}] in the intracellular solution. (B) The average potentiation of TRPC5 current by 100 μM La^{3+}. With 200 nM of calculated free [Ca^{2+}] in the pipette, current at −40 mV was increased 14.53 ± 1.1-fold, and the current at +100 mV was increased 5.53 ± 0.71-fold. With 1.8 μM of calculated free [Ca^{2+}] in the pipette, the current at −40 mV was increased 12.04 ± 2.35-fold, and the current at +100 mV was increased 2.06 ± 0.4-fold. With 100 μM of calculated free [Ca^{2+}] in the pipette, the current at −40 mV was increased 6.07 ± 1.1-fold, and the current at +100 mV was increased 1.55 ± 0.1-fold (n = 5 for each). External solution was nominally Ca free to eliminate competition between Ca^{2+} and La^{3+} for the shared external binding site. Internal solutions: 0.2 μM of calculated free [Ca^{2+}] (in mM): 110 Cs-Asp, 10 CsCl, 2 $MgCl_2$, 10 Cs_4-BAPTA, 4.7 mM $CaCl_2$, 4 MgATP, 0.3 Na-GTP, and 10 HEPES, pH 7.20 with CsOH; 1.8 μM of calculated free [Ca^{2+}] solution (in mM): 150 Cs-Asp, 0.43 $CaCl_2$, 5 HEDTA, 2 $MgCl_2$, 4 MgATP, 0.3 NaGTP, and 10 HEPES, pH 7.20 with CsOH; and 100 μM [Ca^{2+}] solution (in mM): 150 Cs-Asp, 0.10 $CaCl_2$, 2 $MgCl_2$, 4 MgATP, 0.3 NaGTP, and 10 HEPES, pH 7.20 with CsOH. External solutions: 2 Ca and nominally Ca-free externals.

TRPC5 currents on average 12.04-fold at −40 mV and 2.06-fold at +100 mV. Increasing internal [Ca^{2+}] to 100 μM further reduced La^{3+} potentiation of TRPC5 current to 6.07-fold at −40 mV and 1.55-fold at +100 mV. Thus, the reduction in La^{3+} potentiation was voltage dependent, being more pronounced at +100 mV (approximately threefold reduction) than at −40 mV (∼20% reduction) when the internal solution contained 1.8 μM of calculated [Ca^{2+}]. Jung et al. (2003) have demonstrated that the effect of La^{3+} is to increase channel open probability, overcoming direct channel block by La^{3+}. Our single-channel data suggest that a primary feature of internal Ca^{2+} potentiation is also to increase channel open probability, which may occlude the action of La^{3+}.

Calmodulin does not play a role in intracellular Ca^{2+} potentiation of agonist-activated TRPC5 channels

The primary sequence of TRPC5 channels contains three putative calmodulin-binding domains; interactions have been demonstrated at the two carboxy-terminal domains (Zhu, 2005). In one case, calmodulin binding appeared to speed TRPC5 channel activation kinetics (Ordaz et al., 2005). We tested Ca^{2+}/calmodulin's participation in potentiation by including calmodulin inhibitors in the internal solution and by coexpressing dominant-negative calmodulin (Fig. 14).

In the first of two experiments, we included 1 μM of calmodulin inhibitory peptide in a Cs-Asp–based internal solution with 1 mM EGTA and recorded TRPC5 currents after activation by 100 μM CCh. This concentration of calmodulin inhibitory peptide is well above the 7 nM IC_{50} determined in vitro (Torok et al., 1998). From five cells recorded in this way, we found that each had biphasic activation, and the peak current density at −40 mV was −113.3 ± 20.0 pA/pF, similar to control cells (e.g., Fig. 1 C). TRPC5 currents recorded with calmodulin inhibitory peptide activated more slowly than control cells, with an ∼2.5-fold increase in the latency to peak (68.7 ± 7.2 s for control, 160 ± 30.63 s for calmodulin inhibitory peptide; P = 0.0087). We also tested whether the calmodulin inhibitor W-7, applied at 10 μM in the 1-mM EGTA internal solution, was able to inhibit the development of large, biphasic TRPC5 currents activated by 100 μM CCh. From each of four cells recorded with W-7 in the pipette, we observed typical biphasic TRPC5 currents, with the average peak current density at −40 mV of −109.5 ± 32.0 pA/pF. In contrast to the calmodulin inhibitory peptide, W-7 treatment

did not significantly affect the latency to peak (control latency 68.7 ± 7.2 s vs. W-7–treated cells 123.0 ± 36.4 s; P = 0.17). In these experiments, we used bath perfusion to exchange external solutions, likely causing the increased latencies for activation in control cells (compare Fig. 1).

Finally, we coexpressed a dominant-negative calmodulin in which all four Ca^{2+} binding E-F hands were mutant (crucial aspartate residues mutated to alanine) with TRPC5 and M1Rs. Similar to the results obtained with calmodulin inhibitors, CCh-activated currents recorded from these cells exhibited the typical biphasic response (Fig. 14 C), with an average peak density at −40 mV of −189.2 ± 37.2 pA/pF (n = 7). As in control cells (e.g., Fig. 3), removal of external Ca^{2+} in these cells led to an immediate decline in the current, followed by a slower reduction in the current over the next 90–120 s. There was no significant effect on the latency to peak current in these cells (control cells: 38.3 ± 5.5 s, n = 18; dominant negative cells: 31.4 ± 8.7 s, n = 7).

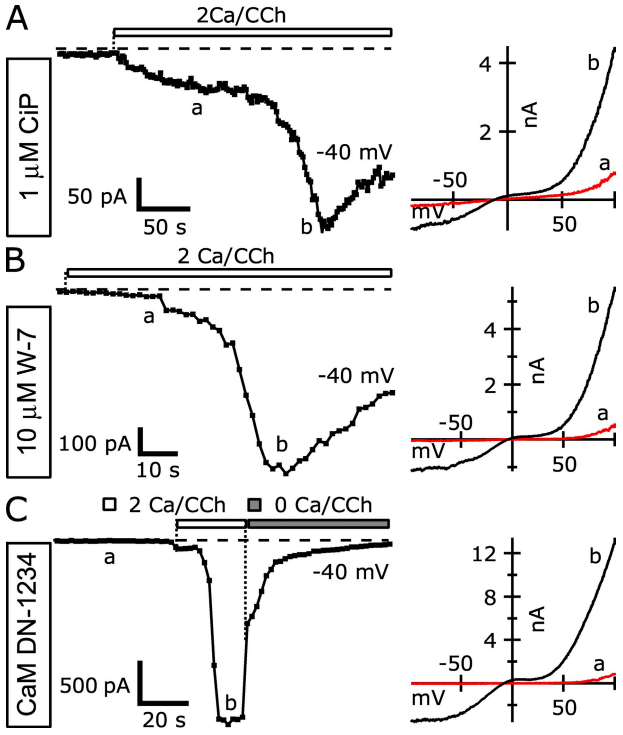

Figure 14. Calmodulin inhibition does not prevent potentiation of TRPC5 by intracellular Ca^{2+}. (A–C; Left) The average currents at −40 mV (squares) recorded from TRPC5 and M1R cotransfected HEK cells during voltage ramps demonstrate Ca^{2+} potentiation in the presence of calmodulin inhibitors. (Right) I-V relations corresponding to points at left indicated by the lowercase letters. (A) Internal 1 μM of calmodulin inhibitory peptide (n = 5). (B) Internal 10 μM W-7 (n = 4). (C) Coexpression of a dominant-negative mutant calmodulin (CaM DN-1234) with TRPC5. Internal Solution (in mM): 150 Cs-Asp, 2 $MgCl_2$, 0.36 $CaCl_2$, 1 EGTA, 4 MgATP, 0.3 NaGTP, and 10 HEPES, pH 7.20 with CsOH (100 nM of calculated free [Ca^{2+}]). External solution: 2 Ca and nominally Ca-free external.

Our results suggest that calmodulin is not involved in the intracellular Ca^{2+} potentiation of TRPC5 channels. Although previous studies have shown that calmodulin inhibitors do not affect TRPC5 current amplitudes (Ordaz et al., 2005), some report that calmodulin inhibitors reduce agonist-activated TRPC5 currents (Kim et al., 2006; Shimizu et al., 2006). These reports suggest that calmodulin acts via myosin light chain kinase to either affect upstream receptor signaling or the plasma membrane delivery of TRPC5 channels. The presence of large, CCh-activated TRPC5 currents in our experiments might result from the overexpression of M1Rs or the use of low [Ca^{2+}] internal buffering.

DISCUSSION

Our results suggest that intracellular [Ca^{2+}] elevations will play an important role in controlling the amplitude of agonist-activated TRPC5 currents. Potentiation of the TRPC5 channel appears to be maximal at [Ca^{2+}] > 1 μM, leading to an ∼25-fold increase in inward currents at physiological membrane potentials. These large current amplitudes could generate a strong membrane depolarization and also further enhance Ca^{2+} entry directly through TRPC5 channels themselves. Furthermore, the intracellular [Ca^{2+}] dependence and the demonstrated ability of heterologously expressed TRPC5 channels to overcome low internal solution buffering conditions must be considered when evaluating mechanisms proposed to modulate TRPC5 activity. This is especially important in Ca^{2+} imaging experiments, when endogenous buffer capacity is unknown. Maintaining constant [Ca^{2+}] levels with high concentrations of internal solution buffers, or removal of external Ca^{2+}, will mitigate the confounding effects of uncontrolled intracellular [Ca^{2+}].

How does intracellular [Ca^{2+}] alter the activity of TRPC5 channels to generate potentiation?

Our results show that changes in the single-channel conductance do not occur during potentiation, suggesting that some combination of increased channel number (N) or channel open probability is likely to be the cause. Although some fraction of TRPC5 channels are located in intracellular vesicles and can be inserted into the plasma membrane in response to activation of growth factor receptors (Bezzerides et al., 2004), the kinetics of that process (∼2.5 min to peak) are much slower than the typical onset of TRPC5 channel potentiation, which had latencies of ∼30 s. Additionally, our single-channel data suggest that the likelihood of an increase in channel number during potentiation in those experiments is very low. Lastly, the voltage dependence of this potentiation (∼5-fold at +100 mV and 25-fold at −40 mV), and its occlusion of external Ca^{2+}/lanthanide potentiation, suggests that changes in channel open

probability likely contribute to the effect. TRPC5 channels are voltage dependent, with depolarization-enhancing activation (Obukhov and Nowycky, 2008). One possibility is that the binding of intracellular Ca^{2+} shifts the position of the voltage dependence of activation toward more hyperpolarized potentials, analogous to the effect of Ca^{2+} on large-conductance Ca^{2+}-activated potassium (i.e., BK) channels (Cui et al., 1997). Such a time-dependent shift in the activation curve, as calcium increases, might also explain the different kinetics of potentiation for outward and inward current (Fig. 1 B). For example, if the current at +100 mV begins with a nonzero extent of activation, whereas the current at −40 mV begins at the foot of the activation curve, a hyperpolarizing shift in the activation curve will immediately result in increased current at +100 mV, whereas the current at −40 mV will activate with a delay. Such an explanation has been suggested for TRPV1 activation by capsaicin and TRPM8 activation by menthol (Voets et al., 2004). Lastly, the binding of extracellular Ca^{2+}/lanthanides might result in a similar shift in the voltage dependence of activation, causing the observed voltage-dependent increase in TRPC5 channel open probability, as suggested by Obukhov and Nowycky (2008).

Where does Ca^{2+} bind to potentiate agonist-activated TRPC5 channels?

The precise location where calcium acts to potentiate TRPC5 channels is not completely clear from our experiments. A location close to, or perhaps directly on, the channel is supported by the greater effectiveness of 10 mM BAPTA relative to 10 mM EGTA in preventing potentiation (Fig. 2 B). A more distant location is supported by several results, including the dependence of TRPC5 potentiation on global [Ca^{2+}], as directly measured by fura-2 (Fig. 5); the ability of 10 mM EGTA to slow, and in some cells prevent, potentiation (Fig. 2 A); and the slow decline in TRPC5 current after the removal of external calcium (Fig. 3). Furthermore, the persistence of potentiation in some excised patches suggests that the mechanism can survive removal from the cell. Lacking detailed information on the contribution of calcium ions to the overall TRPC5 current, as well as uncertainties stemming from buffer saturation and varying channel expression level, it is difficult to model the profile of [Ca^{2+}] near open TRPC5 channels. What is clear is that the Ca^{2+} entering through a single TRPC5 channel is insufficient to generate potentiation, or else we would have observed it in every cell. Similarly, we would not have observed potentiation of TRPC5 channels in our cell-attached recordings (where the pipette contained 2 Ca external solution) after the addition of 10 Ca solution to the bath (Fig. 10 A). This dependence on calcium arising from more distant TRPC5 channels might possibly lead to the correlation between global [Ca^{2+}] and potentiation, even with a sensor location associated with the channel (yet still relatively distant from the channel mouth).

There are no predicted Ca^{2+} binding sites on TRPC5 channels, but there are three motifs suggested to interact with calmodulin or related Ca^{2+} binding proteins. One is located in the amino terminus, and two are in the carboxy terminus (Zhu, 2005). Ordaz et al. (2005) showed that calmodulin binding to the second carboxy-terminal domain, called CBII (amino acids 828–854 of mouse TRPC5), results in faster agonist activation of TRPC5 currents, but leaves maximal current amplitudes unchanged. This observation is consistent with our result that inhibition of calmodulin does not affect Ca^{2+} potentiation (Fig. 14). Ca^{2+} binding protein 1 has also been reported to bind the carboxy terminus of TRPC5 (over a larger region), although its inhibition of Ca^{2+} activation of TRPC5 channels makes it unlikely to act as the sensor for potentiation (Kinoshita-Kawada et al., 2005).

NCS-1 is another Ca^{2+} binding protein that has effects on Ca_V, K_V, and IP_3 receptor channels (for review see Burgoyne, 2007). NCS-1 has been shown to interact with TRPC5, again in the carboxy-terminal region (Hui et al., 2006). They showed that coexpression of a dominant-negative E-F hand mutant of NCS-1 reduced TRPC5 activity in response to muscarinic receptor activation, extracellular lanthanides, or intracellular Ca^{2+}, but not through changes in surface TRPC5 expression. NCS-1 is a possible candidate underlying Ca^{2+} potentiation, though it is unknown whether NCS-1 interacts with TRPC4β, which can also be potentiated.

Ca^{2+} has myriad effects on TRP channels and GPCR/PLC signaling pathways

Ca^{2+} plays a central role in controlling the activity of many TRP channels, either through direct binding to the channel or through the effects of Ca^{2+} binding proteins, such as calmodulin (for review see Zhu, 2005). For example, TRPA1 is strongly potentiated by intracellular Ca^{2+}, which may bind at the E-F hand motif located in the amino terminus of the channel (Doerner et al., 2007; Zurborg et al., 2007; Wang et al., 2008). Calmodulin interacts directly with many TRP channels to effect both positive and negative regulation; examples include *Drosophila* TRPL (Zimmer et al., 2000), TRPC6 and TRPC7 (Shi et al., 2004), TRPV1 (Rosenbaum et al., 2004), TRPV3 (Xiao et al., 2008), TRPV4 (Strotmann et al., 2003), TRPV6 (Lambers et al., 2004), TRPM2 (Tong et al., 2006), and TRPM4 (Nilius et al., 2005).

When using GPCR stimulation to activate TRP channels, it should be noted that numerous steps before channel activation are Ca^{2+} or calmodulin dependent, including receptor desensitization (Mundell et al., 2004; Turner and Raymond, 2005), PLC activation (McCullar et al., 2003; Horowitz et al., 2005), and PKC activation. Calmodulin regulation of components in the upstream activation pathways of some channels can lead to changes

in agonist-activated current amplitudes. For example, calmodulin mutant alleles strongly reduce the light-activated currents of TRPL channels but leave quantal bumps unaffected, suggesting that the channels themselves remain functional (Scott et al., 1997). Another example is TRPC5 itself; application of calmodulin inhibitors reduces M1R-activated currents (presumably via myosin light chain kinase) but spares currents activated by intracellular perfusion of GTPγS (bypassing the receptor pathway) (Kim et al., 2006; see also Shimizu et al., 2006).

Potential physiological roles of TRPC4 and TRPC5 potentiation by intracellular Ca^{2+}

The properties of TRPC4 and TRPC5 channels share many similarities with a muscarinic receptor–activated cation current recorded in several different gastrointestinal smooth muscle cell types. The muscarinic-activated cation current in these cells has an I-V relation that is inwardly rectifying and flat positive to the reversal potential (Inoue and Isenberg, 1990a), is activated by depolarization (Inoue and Isenberg, 1990b; Zholos and Bolton, 1994), and is potentiated by external La^{3+} (Inoue et al., 1998). Inoue and Isenberg (1990c) have demonstrated that this current, recorded from guinea pig ileum, is also potentiated by intracellular Ca^{2+} with an EC_{50} of ~200 nM, and that this potentiation was maximal at >1 μM. In comparison, our results showed that $[Ca^{2+}] > 350$ nM was required to generate potentiation, which was maximal at 1.4 μM $[Ca^{2+}]$. Expression analysis suggests that TRPC4 is more likely to produce the ileal smooth muscle cell muscarinic-activated cation current (Lee et al., 2003; Lee et al., 2005). If true, the higher Ca^{2+} sensitivity of this current might reflect an intrinsic difference between TRPC4 and TRPC5 channels or, alternatively, modulation by endogenous mechanisms.

The muscarinic-activated current depolarizes smooth muscle cells to trigger Ca_V channels, and the resulting Ca^{2+} entry then feeds back to potentiate the cation current, prolonging the depolarization. In contrast, Ca^{2+} entering through TRPC5 channels themselves was the likely source of intracellular $[Ca^{2+}]$ elevations in our experiments. This suggests that any $[Ca^{2+}]$ elevation, resulting either from Ca^{2+} entry (via Ca_V or Ca^{2+}-permeable neurotransmitter-gated channels) or release from internal stores, that reaches a sufficient level can be integrated by TRPC4 and TRPC5 channels and alter their activity.

TRPC5 is expressed in a variety of brain regions, including neurons in the hippocampus, cortex, amygdala, cerebellum, and hypothalamus (Mori et al., 1998; Philipp et al., 1998; Strubing et al., 2001; Fowler et al., 2007). The precise roles of TRPC5 channels in these neuronal cell types remain undefined, although they are excellent candidates for generating nonselective cation currents activated by metabotropic glutamate receptors (Fowler et al., 2007) or neuropeptides (Meis et al., 2007; Kohlmeier et al., 2008). Furthermore, Ca^{2+}-dependent nonselective cation currents have been described in neurons from the substantia nigra (Lee and Tepper, 2007) and the entorhinal cortex (Magistretti et al., 2004), but the source of the $[Ca^{2+}]$ required to activate these currents is unknown. These currents may be generated by TRPC4 or TRPC5 channels, or by other Ca^{2+}-sensitive TRP channels. The typically small amplitude of most neuronal nonselective currents, in the presence of multiple endogenous conductances, makes testing their properties difficult. Such studies might be facilitated by manipulations that increase $[Ca^{2+}]$ to maximize TRP channel potentiation.

Resting $[Ca^{2+}]$ in most neurons is typically ~50–150 nM, but repetitive activity and back-propagating action potentials can generate $[Ca^{2+}]$ elevations of ~0.2 to >1 μM in dendrites and dendritic spines via activation of Ca_V channels (e.g., Helmchen et al., 1996; Sabatini et al., 2002). Activation of NMDA receptors can generate even higher levels, >10 μM in spines (Petrozzino et al., 1995). These $[Ca^{2+}]$ would be sufficient to potentiate TRPC5 channels when occurring simultaneously with GPCR activation and, again, enhance depolarization and Ca^{2+} entry.

Although the subcellular localization of TRPC5 channels in adult neurons is unknown, TRPC5 is expressed throughout the soma and processes, including growth cones, of embryonic hippocampal neurons (Greka et al., 2003). Ca^{2+} is critically important in controlling growth cone motility (for review see Gomez and Zheng, 2006), and Ca_V channels, internal stores, and receptor-activated channels all contribute to growth cone $[Ca^{2+}]$. The Ca^{2+}-dependent potentiation of TRPC5 might make it a crucial integrator of these multiple signals.

We thank the members of the Clapham laboratory for helpful comments and Svetlana Gapon for tissue culture. The dominant-negative calmodulin plasmid was provided by David T. Yue, and the TRPC4β plasmid was provided by Louis H. Philipson.

Angus C. Nairn served as editor.

Submitted: 31 October 2008
Accepted: 13 April 2009

REFERENCES

Bezzerides, V.J., I.S. Ramsey, S. Kotecha, A. Greka, and D.E. Clapham. 2004. Rapid vesicular translocation and insertion of TRP channels. *Nat. Cell Biol.* 6:709–720.

Biddlecome, G.H., G. Berstein, and E.M. Ross. 1996. Regulation of phospholipase C-beta1 by Gq and m1 muscarinic cholinergic receptor. Steady-state balance of receptor-mediated activation and GTPase-activating protein-promoted deactivation. *J. Biol. Chem.* 271:7999–8007.

Burgoyne, R.D. 2007. Neuronal calcium sensor proteins: generating diversity in neuronal Ca^{2+} signalling. *Nat. Rev. Neurosci.* 8:182–193.

Chung, M.K., A.D. Guler, and M.J. Caterina. 2005. Biphasic currents evoked by chemical or thermal activation of the heat-gated ion channel, TRPV3. *J. Biol. Chem.* 280:15928–15941.

Chung, M.K., A.D. Guler, and M.J. Caterina. 2008. TRPV1 shows dynamic ionic selectivity during agonist stimulation. *Nat. Neurosci.* 11:555–564.

Colquhoun, D., and A.G. Hawkes. 1995. The principles of the stochastic interpretation of ion-channel mechanisms. *In* Single-Channel Recording. B. Sakmann and E. Neher, editors. Plenum Press, New York and London. 397–482.

Cui, J., D.H. Cox, and R.W. Aldrich. 1997. Intrinsic voltage dependence and Ca^{2+} regulation of *mslo* large conductance Ca-activated K^+ channels. *J. Gen. Physiol.* 109:647–673.

Dattilo, M., N.J. Penington, and K. Williams. 2008. Inhibition of TRPC5 channels by intracellular ATP. *Mol. Pharmacol.* 73: 42–49.

Doerner, J.F., G. Gisselmann, H. Hatt, and C.H. Wetzel. 2007. Transient receptor potential channel A1 is directly gated by calcium ions. *J. Biol. Chem.* 282:13180–13189.

Drin, G., and S. Scarlata. 2007. Stimulation of phospholipase Cbeta by membrane interactions, interdomain movement, and G protein binding–how many ways can you activate an enzyme? *Cell. Signal.* 19:1383–1392.

Fowler, M.A., K. Sidiropoulou, E.D. Ozkan, C.W. Phillips, and D.C. Cooper. 2007. Corticolimbic expression of TRPC4 and TRPC5 channels in the rodent brain. *PLoS One.* 2:e573.

Gomez, T.M., and J.Q. Zheng. 2006. The molecular basis for calcium-dependent axon pathfinding. *Nat. Rev. Neurosci.* 7:115–125.

Greka, A., B. Navarro, E. Oancea, A. Duggan, and D.E. Clapham. 2003. TRPC5 is a regulator of hippocampal neurite length and growth cone morphology. *Nat. Neurosci.* 6:837–845.

Hardie, R.C. 2005. Inhibition of phospholipase C activity in Drosophila photoreceptors by 1,2-bis(2-aminophenoxy)ethane N,N,N',N'-tetraacetic acid (BAPTA) and di-bromo BAPTA. *Cell Calcium.* 38:547–556.

Hartmann, J., E. Dragicevic, H. Adelsberger, H.A. Henning, M. Sumser, J. Abramowitz, R. Blum, A. Dietrich, M. Freichel, V. Flockerzi, et al. 2008. TRPC3 channels are required for synaptic transmission and motor coordination. *Neuron.* 59:392–398.

Helmchen, F., K. Imoto, and B. Sakmann. 1996. Ca^{2+} buffering and action potential-evoked Ca^{2+} signaling in dendrites of pyramidal neurons. *Biophys. J.* 70:1069–1081.

Hofmann, T., M. Schaefer, G. Schultz, and T. Gudermann. 2002. Subunit composition of mammalian transient receptor potential channels in living cells. *Proc. Natl. Acad. Sci. USA.* 99:7461–7466.

Horowitz, L.F., W. Hirdes, B.C. Suh, D.W. Hilgemann, K. Mackie, and B. Hille. 2005. Phospholipase C in living cells: activation, inhibition, Ca^{2+} requirement, and regulation of M current. *J. Gen. Physiol.* 126:243–262.

Hui, H., D. McHugh, M. Hannan, F. Zeng, S.Z. Xu, S.U. Khan, R. Levenson, D.J. Beech, and J.L. Weiss. 2006. Calcium-sensing mechanism in TRPC5 channels contributing to retardation of neurite outgrowth. *J. Physiol.* 572:165–172.

Inoue, R., and G. Isenberg. 1990a. Acetylcholine activates nonselective cation channels in guinea pig ileum through a G protein. *Am. J. Physiol.* 258:C1173–C1178.

Inoue, R., and G. Isenberg. 1990b. Effect of membrane potential on acetylcholine-induced inward current in guinea-pig ileum. *J. Physiol.* 424:57–71.

Inoue, R., and G. Isenberg. 1990c. Intracellular calcium ions modulate acetylcholine-induced inward current in guinea-pig ileum. *J. Physiol.* 424:73–92.

Inoue, R., H. Morita, H. Yanagida, and Y. Ito. 1998. Potentiating actions of lanthanum on ACh-induced cation current in guinea-pig ileal smooth muscle cells. *J. Smooth Muscle Res.* 34:69–81.

Jung, S., A. Muhle, M. Schaefer, R. Strotmann, G. Schultz, and T.D. Plant. 2003. Lanthanides potentiate TRPC5 currents by an action at extracellular sites close to the pore mouth. *J. Biol. Chem.* 278:3562–3571.

Kim, M.T., B.J. Kim, J.H. Lee, S.C. Kwon, D.S. Yeon, D.K. Yang, I. So, and K.W. Kim. 2006. Involvement of calmodulin and myosin light chain kinase in activation of mTRPC5 expressed in HEK cells. *Am. J. Physiol. Cell Physiol.* 290:C1031–C1040.

Kim, S.J., Y.S. Kim, J.P. Yuan, R.S. Petralia, P.F. Worley, and D.J. Linden. 2003. Activation of the TRPC1 cation channel by metabotropic glutamate receptor mGluR1. *Nature.* 426:285–291.

Kinoshita-Kawada, M., J. Tang, R. Xiao, S. Kaneko, J.K. Foskett, and M.X. Zhu. 2005. Inhibition of TRPC5 channels by Ca^{2+}-binding protein 1 in Xenopus oocytes. *Pflugers Arch.* 450:345–354.

Kohlmeier, K.A., S. Watanabe, C.J. Tyler, S. Burlet, and C.S. Leonard. 2008. Dual orexin actions on dorsal raphe and laterodorsal tegmentum neurons: noisy cation current activation and selective enhancement of Ca^{2+} transients mediated by L-type calcium channels. *J. Neurophysiol.* 100:2265–2281.

Lambers, T.T., A.F. Weidema, B. Nilius, J.G. Hoenderop, and R.J. Bindels. 2004. Regulation of the mouse epithelial Ca2(+) channel TRPV6 by the $Ca^{(2+)}$-sensor calmodulin. *J. Biol. Chem.* 279:28855–28861.

Lee, C.R., and J.M. Tepper. 2007. A calcium-activated nonselective cation conductance underlies the plateau potential in rat substantia nigra GABAergic neurons. *J. Neurosci.* 27:6531–6541.

Lee, K.P., J.Y. Jun, I.Y. Chang, S.H. Suh, I. So, and K.W. Kim. 2005. TRPC4 is an essential component of the nonselective cation channel activated by muscarinic stimulation in mouse visceral smooth muscle cells. *Mol. Cells.* 20:435–441.

Lee, Y.M., B.J. Kim, H.J. Kim, D.K. Yang, M.H. Zhu, K.P. Lee, I. So, and K.W. Kim. 2003. TRPC5 as a candidate for the nonselective cation channel activated by muscarinic stimulation in murine stomach. *Am. J. Physiol. Gastrointest. Liver Physiol.* 284:G604–G616.

Magistretti, J., L. Ma, M.H. Shalinsky, W. Lin, R. Klink, and A. Alonso. 2004. Spike patterning by Ca^{2+}-dependent regulation of a muscarinic cation current in entorhinal cortex layer II neurons. *J. Neurophysiol.* 92:1644–1657.

McCullar, J.S., S.A. Larsen, R.A. Millimaki, and T.M. Filtz. 2003. Calmodulin is a phospholipase C-beta interacting protein. *J. Biol. Chem.* 278:33708–33713.

Meis, S., T. Munsch, L. Sosulina, and H.C. Pape. 2007. Postsynaptic mechanisms underlying responsiveness of amygdaloid neurons to cholecystokinin are mediated by a transient receptor potential-like current. *Mol. Cell. Neurosci.* 35:356–367.

Mori, Y., N. Takada, T. Okada, M. Wakamori, K. Imoto, H. Wanifuchi, H. Oka, A. Oba, K. Ikenaka, and T. Kurosaki. 1998. Differential distribution of TRP Ca^{2+} channel isoforms in mouse brain. *Neuroreport.* 9:507–515.

Mundell, S.J., G. Pula, R.A. McIlhinney, P.J. Roberts, and E. Kelly. 2004. Desensitization and internalization of metabotropic glutamate receptor 1a following activation of heterologous Gq/11-coupled receptors. *Biochemistry.* 43:7541–7551.

Naraghi, M. 1997. T-jump study of calcium binding kinetics of calcium chelators. *Cell Calcium.* 22:255–268.

Neher, E. 1998. Vesicle pools and Ca^{2+} microdomains: new tools for understanding their roles in neurotransmitter release. *Neuron.* 20:389–399.

Neher, E. 2005. Some quantitative aspects of calcium fluorimetry. *In* Imaging in Neuroscience and Development. R. Yuste and A. Konnerth, editors. Cold Spring Harbor Laboratory Press, Cold Spring Harbor, NY. 245–252.

Nilius, B., J. Prenen, J. Tang, C. Wang, G. Owsianik, A. Janssens, T. Voets, and M.X. Zhu. 2005. Regulation of the Ca^{2+} sensitivity of the nonselective cation channel TRPM4. *J. Biol. Chem.* 280:6423–6433.

Obukhov, A.G., and M.C. Nowycky. 2004. TRPC5 activation kinetics are modulated by the scaffolding protein ezrin/radixin/moesin-binding phosphoprotein-50 (EBP50). *J. Cell. Physiol.* 201:227–235.

Obukhov, A.G., and M.C. Nowycky. 2005. A cytosolic residue mediates Mg^{2+} block and regulates inward current amplitude of a transient receptor potential channel. *J. Neurosci.* 25:1234–1239.

Obukhov, A.G., and M.C. Nowycky. 2008. TRPC5 channels undergo changes in gating properties during the activation-deactivation cycle. *J. Cell. Physiol.* 216:162–171.

Okada, T., S. Shimizu, M. Wakamori, A. Maeda, T. Kurosaki, N. Takada, K. Imoto, and Y. Mori. 1998. Molecular cloning and functional characterization of a novel receptor-activated TRP Ca^{2+} channel from mouse brain. *J. Biol. Chem.* 273:10279–10287.

Ordaz, B., J. Tang, R. Xiao, A. Salgado, A. Sampieri, M.X. Zhu, and L. Vaca. 2005. Calmodulin and calcium interplay in the modulation of TRPC5 channel activity. Identification of a novel C-terminal domain for calcium/calmodulin-mediated facilitation. *J. Biol. Chem.* 280:30788–30796.

Otsuguro, K., J. Tang, Y. Tang, R. Xiao, M. Freichel, V. Tsvilovskyy, S. Ito, V. Flockerzi, M.X. Zhu, and A.V. Zholos. 2008. Isoform-specific inhibition of TRPC4 channel by phosphatidylinositol 4,5-bisphosphate. *J. Biol. Chem.* 283:10026–10036.

Petrozzino, J.J., L.D. Pozzo Miller, and J.A. Connor. 1995. Micromolar Ca^{2+} transients in dendritic spines of hippocampal pyramidal neurons in brain slice. *Neuron.* 14:1223–1231.

Philipp, S., J. Hambrecht, L. Braslavski, G. Schroth, M. Freichel, M. Murakami, A. Cavalie, and V. Flockerzi. 1998. A novel capacitative calcium entry channel expressed in excitable cells. *EMBO J.* 17:4274–4282.

Plant, T.D., and M. Schaefer. 2005. Receptor-operated cation channels formed by TRPC4 and TRPC5. *Naunyn Schmiedebergs Arch. Pharmacol.* 371:266–276.

Ramsey, I.S., M. Delling, and D.E. Clapham. 2006. An introduction to TRP channels. *Annu. Rev. Physiol.* 68:619–647.

Rosenbaum, T., A. Gordon-Shaag, M. Munari, and S.E. Gordon. 2004. Ca^{2+}/calmodulin modulates TRPV1 activation by capsaicin. *J. Gen. Physiol.* 123:53–62.

Sabatini, B.L., T.G. Oertner, and K. Svoboda. 2002. The life cycle of $Ca^{(2+)}$ ions in dendritic spines. *Neuron.* 33:439–452.

Schaefer, M., T.D. Plant, A.G. Obukhov, T. Hofmann, T. Gudermann, and G. Schultz. 2000. Receptor-mediated regulation of the nonselective cation channels TRPC4 and TRPC5. *J. Biol. Chem.* 275:17517–17526.

Schaefer, M., T.D. Plant, N. Stresow, N. Albrecht, and G. Schultz. 2002. Functional differences between TRPC4 splice variants. *J. Biol. Chem.* 277:3752–3759.

Scott, K., Y. Sun, K. Beckingham, and C.S. Zuker. 1997. Calmodulin regulation of Drosophila light-activated channels and receptor function mediates termination of the light response in vivo. *Cell.* 91:375–383.

Shi, J., E. Mori, Y. Mori, M. Mori, J. Li, Y. Ito, and R. Inoue. 2004. Multiple regulation by calcium of murine homologues of transient receptor potential proteins TRPC6 and TRPC7 expressed in HEK293 cell. *J. Physiol.* 561:415–432.

Shimizu, S., T. Yoshida, M. Wakamori, M. Ishii, T. Okada, M. Takahashi, M. Seto, K. Sakurada, Y. Kiuchi, and Y. Mori. 2006. Ca^{2+}-calmodulin-dependent myosin light chain kinase is essential for activation of TRPC5 channels expressed in HEK293 cells. *J. Physiol.* 570:219–235.

Strotmann, R., G. Schultz, and T.D. Plant. 2003. Ca^{2+}-dependent potentiation of the nonselective cation channel TRPV4 is mediated by a C-terminal calmodulin binding site. *J. Biol. Chem.* 278:26541–26549.

Strubing, C., G. Krapivinsky, L. Krapivinsky, and D.E. Clapham. 2001. TRPC1 and TRPC5 form a novel cation channel in mammalian brain. *Neuron.* 29:645–655.

Strubing, C., G. Krapivinsky, L. Krapivinsky, and D.E. Clapham. 2003. Formation of novel TRPC channels by complex subunit interactions in embryonic brain. *J. Biol. Chem.* 278:39014–39019.

Tong, Q., W. Zhang, K. Conrad, K. Mostoller, J.Y. Cheung, B.Z. Peterson, and B.A. Miller. 2006. Regulation of the transient receptor potential channel TRPM2 by the Ca^{2+} sensor calmodulin. *J. Biol. Chem.* 281:9076–9085.

Torok, K., D.J. Cowley, B.D. Brandmeier, S. Howell, A. Aitken, and D.R. Trentham. 1998. Inhibition of calmodulin-activated smooth-muscle myosin light-chain kinase by calmodulin-binding peptides and fluorescent (phosphodiesterase-activating) calmodulin derivatives. *Biochemistry.* 37:6188–6198.

Turner, J.H., and J.R. Raymond. 2005. Interaction of calmodulin with the serotonin 5-hydroxytryptamine2A receptor. A putative regulator of G protein coupling and receptor phosphorylation by protein kinase C. *J. Biol. Chem.* 280:30741–30750.

Venkatachalam, K., and C. Montell. 2007. TRP channels. *Annu. Rev. Biochem.* 76:387–417.

Voets, T., G. Droogmans, U. Wissenbach, A. Janssens, V. Flockerzi, and B. Nilius. 2004. The principle of temperature-dependent gating in cold- and heat-sensitive TRP channels. *Nature.* 430:748–754.

Wang, Y.Y., R.B. Chang, H.N. Waters, D.D. McKemy, and E.R. Liman. 2008. The nociceptor ion channel TRPA1 is potentiated and inactivated by permeating calcium ions. *J. Biol. Chem.* 283:32691–32703.

Willars, G.B., S.R. Nahorski, and R.A. Challiss. 1998. Differential regulation of muscarinic acetylcholine receptor-sensitive polyphosphoinositide pools and consequences for signaling in human neuroblastoma cells. *J. Biol. Chem.* 273:5037–5046.

Xiao, R., J. Tang, C. Wang, C.K. Colton, J. Tian, and M.X. Zhu. 2008. Calcium plays a central role in the sensitization of TRPV3 channel to repetitive stimulations. *J. Biol. Chem.* 283:6162–6174.

Yamada, H., M. Wakamori, Y. Hara, Y. Takahashi, K. Konishi, K. Imoto, and Y. Mori. 2000. Spontaneous single-channel activity of neuronal TRP5 channel recombinantly expressed in HEK293 cells. *Neurosci. Lett.* 285:111–114.

Zholos, A.V., and T.B. Bolton. 1994. G-protein control of voltage dependence as well as gating of muscarinic metabotropic channels in guinea-pig ileum. *J. Physiol.* 478:195–202.

Zhu, M.H., M. Chae, H.J. Kim, Y.M. Lee, M.J. Kim, N.G. Jin, D.K. Yang, I. So, and K.W. Kim. 2005. Desensitization of canonical transient receptor potential channel 5 by protein kinase C. *Am. J. Physiol. Cell Physiol.* 289:C591–C600.

Zhu, M.X. 2005. Multiple roles of calmodulin and other $Ca^{(2+)}$-binding proteins in the functional regulation of TRP channels. *Pflugers Arch.* 451:105–115.

Zimmer, S., C. Trost, U. Wissenbach, S. Philipp, M. Freichel, V. Flockerzi, and A. Cavalie. 2000. Modulation of recombinant transient-receptor-potential-like (TRPL) channels by cytosolic Ca^{2+}. *Pflugers Arch.* 440:409–417.

Zurborg, S., B. Yurgionas, J.A. Jira, O. Caspani, and P.A. Heppenstall. 2007. Direct activation of the ion channel TRPA1 by Ca^{2+}. *Nat. Neurosci.* 10:277–279.